Supplementary Material

1 SUPPLEMENTARY INFORMATION

1.1 iFEED checklist against recommendations of Challinor et al. (2018)

A score out of 4 is given for each criterion below. A score of 1 indicates no effort being made to address criterion aims. A score of 2 indicates a limited effort with substantial room for improvement in addressing the criterion aims. A score of 3 indicates a good effort, with minor improvements possible. A score of 4 indicates an excellent effort that is unlikely to be improved upon given current limitations. These scores are used to point towards limitations in methods and improvements for further research, as summarised in the discussion.

1. The crop model used, and the processes simulated, should be of appropriate complexity given the evidence from available data and the spatial scale of the simulations – (3/4)

iFEED does not rely on integrated assessment models due to a desire to make results as easily interpretable as possible – relying on qualitative trade analysis rather than equilibrium models.

GLAM was selected as a crop model precisely because it has been developed for use in large scale (several kilometres squared) simulations – at the spatial scale of the input weather-yield relationship (Challinor et al., 2003, 2004). Recent developments in crop modelling suggest possible simpler (and potentially more skilful) methods, relying on fewer empirically-derived parameters that would further enhance the simplicity and therefore utility of the model (Droutsas et al., 2019).

Gap-filling, as described in the main paper, is used to fill gaps in crops not explicitly simulated. In the discussion we outline the benefits and negatives of using such an approach. On balance, we feel as though this is an approach of justifiable complexity, although given more time more crops could have been included to provide a broader picture of climate impacts – for example, inclusion of representative fruit and vegetable crops, enabling e.g. cereal, root / tuber, fruit / vegetable crop representations, rather than just the C3 / C4 distinction, as used in this study and in Müller and Robertson (2014).

Emissions are modelled using a global version of the ECOSSE model, designed for gridded simulations.

A score of 3 is given as the crop model used is of appropriate complexity for the scale simulated, however the gap-filling but could be improved upon with more time to include a broader range of important crops.

2. Ensembles should be formed from a well-justified set of models and input data (2/4)

Only one crop model was used in this analysis; however, this was reflected in the confidence assessment stage by downgrading confidence in outcomes where necessary. An ensemble of 18 bias-corrected global climate models was used as input into iFEED. This ensemble was selected from the data of Famien et al. (2018). Models with both RCP2.6 and RCP8.5 that had 365 days of daily data were selected from the wider ensemble of 29 models.

For parts of the iFEED analysis, a further subset of 5 models was selected due to computational and methodological constraints. This allowed greater speed of analysis, but comes at the expense of including the full range of climate responses. Careful selection of the subset was undertaken however, using the methods of Ruane and McDermid (2017) (see Section 1.5).

A score of 2 is given. An ensemble of climate inputs is used, however only one crop model and soil input data set is used. Whilst the iFEED approach to summarise results includes confidence statements that reflect this, improvements could be made in the area of ensemble modelling.

3. Bias correction of climate model data should always be carried out, unless the bias is provably small (3/4)

Input data were bias-corrected as detailed in Famien et al. (2018), whose evaluation proved this to be effective at removing bias over West Africa. Evaluation of the bias-correction has not been conducted in the sub-Saharan Africa region in which iFEED is applied however. A score of 3 is therefore given.

4. Projections should include uncertainty estimates. The method for quantifying uncertainty should permit assessment of the realism of the resulting ranges (3/4)

Model results are associated with uncertainty associated with climate model inputs – usually displayed as a range of percentage change in output variables such as yield, production, or emissions relative to the baseline. However, this underlying uncertainty is associate with climate model inputs rather than other sources of input data also.

The calibrated statement process allows a more comprehensive assessment of the uncertainty associated with projections. Rather than simply relying on the uncertainty associated with climate model inputs, each aspect of the modelling is assessed in terms of its robustness to possible changes in model assumptions or parameters, as well as assessing agreement with broader literature. This gives a more complete picture of the realism of results. Hence, a score of 3 is given, as whilst more models and input data could form a more complete quantification of uncertainty, the calibrated statement process effectively includes all of these considerations.

5.The model used should be evaluated using historical observed data (3/4)

The crop model underlying iFEED analysis was evaluated using FAOSTAT data. In the absence of more detailed data on crop phenology and growth in the region, these yield data provide adequate assessment of how well the model simulates the inter-annual variability of yield. Where relationships between yield and climate exists, GLAM generally is shown to effectively capture this, as can be seen in the SI. A score of 3 is given for this reason, as further data could help to evaluate GLAM, such as biomass, sowing and harvest data, although these are hard to come by at national scales.

6. Model projections and methodologies should be critically evaluated and the limitations of the study made explicit (4/4)

The calibrated statement process details limitations to certainty in conclusions. In addition, this section explicitly highlights important limitations and strengths. A score of 4 is therefore given.

7. The assumptions underlying the results of the study should be explicit. A common uncertainty reporting format can be used to achieve this (4/4)

This supplemntary information details any important assumptions behind iFEED modelling. In addition, as described under heading 4, the calibrated statement process provides a common uncertainty reporting format that takes into account any key assumptions and reflects these in certainty of conclusions. A score of 4 is therefore given.

8. Assessments of climate change impacts should include autonomous adaptation; otherwise impacts will likely be over-estimated (4/4)

Autonomous adaptation is the default assumption in iFEED crop model projections. Certain scenarios assume more optimistic adaptation of crop varieties that mitigate against growing season duration reduction or have improved irrigation.

The effect of any future adaptations is compared directly to historical counterparts, with both periods using the same method of selecting planting dates and crop varieties. We thus avoid the "adaptation illusion" highlighted by Lobell (2014), whereby adaptation tends to be over-estimated by the common practice of comparing a non-adapted historical period with an adapted future period.

A maximum score of 4 is therefore given.

9. The simulations carried out should be documented in sufficient detail to demonstrate the extent to which the above criteria have been met, and to ensure reproducibility of the work carried out. (4/4)

The methods detailed in this paper and the discussion section detail this, therefore 4 out of 4.

Additional criteria for adaptation studies and risk assessments:

1. Assessments of risk need broad system boundaries (3/4)

The choice of system boundary is the national scale for iFEED, although recognition of the broader nature of trade is important, and is encompassed by the trade component of the analysis. More explicit incorporation of the international nature of trade is possible, hence 3 out of 4.

2. Engagement with stakeholders is critical if the research aims to have a practical risk management or adaptation outcome (4/4)

Stakeholder input is key to every stage of iFEED, from the initial design of scenarios to modelling them to results orientation and presentation. A score of 4 is given because of these efforts.

1.2 iFEED yield projetions - gapfill and trends

Similarly to Müller and Robertson (2014), crop yield projections were averaged to represent all crops with growing area in baseline period according to FAO (2019). A total of 92 commodities across the four countries were included in the analysis. Methods for this process were as follows:

1. Average the relevant crops (e.g. potato, groundnut and soybean as C3 crops. Note that maize used as gap-filling crop for millet, sugarcane and sorghum - for sugarcane, climate change impacts on maize biomass are used) for baseline (1990-2010) and future (2040-2060) yields. Note each crop yield is first normalised to ensure an even crop contribution (in terms of climate change impact) to the average for gap-filling. Median rather than mean is used to normalise so high-yielding grid cells do not skew the average, and the same correction is applied to baseline and future to not interfere with climate impacts.
2. Average national FAO yields from 1990-2010 for each commodity.
3. Calculate a national simulated yield for the year 2000 using grid cell area information for the crop in question (from LUH2/FAO) and the gridded mean C3 yields, averaged for the baseline period (add up total area nationally, and total production at each grid cell added to give a national total, and then divide national production by national area).
4. Weight the national simulated mean yields in baseline so they match the mean FAO yield (divide one by the other) and apply this weighting to all grid-cell level yields.
5. Apply the same weighting to future yields.

6. Apply trends (calculated as described below) to each grid cell yield value (50% trends also applied for use in South African scenarios).
7. Check if future trend-applied yields are above the maximum global FAO country-level mean yield for that crop and cap if so by dividing mean future yields by FAO yield and applying this correction factor to the future yields.
8. For the simulated crops maize, soybean, groundnut and potato, if the weighted and trend-applied yields are above potential yields (i.e. YGP = 1 yields), we cap them at the grid cell level to the potential yield value (this in addition to the FAO yield cap check in step 7).

How applied yield trends are calculated:

1. FAOSTAT data from 1961 to 2010 used for all 92 commodities and the four AFRICAP countries used to calculate 10-year averages from 1961-1970 and 2001-2010. This requires at least 3 years of data in each 10 year period, otherwise a country is put to a no data value.
2. Calculate the percentage difference between the start and end 10 year averages for each crop and country.
3. The maximum percentage difference for each crop from amongst the four countries is used for that commodity.
4. If there is insufficient data for any crop and country, or if the maximum trend is negative (i.e. yields are reduced in the region for any commodity), the mean trend across all commodities is used, excluding any negative trends.

1.3 iFEED land use methods

For the future scenarios where agricultural land use was optimised to maximise crop production, the method for deciding future agricultural land use (which crops are grown where, and pasture requirements) is as follows:

1. Prescribe conditions for future land use based on stakeholder recomendations (how much will arable cropland and pasture for livestock increase/decrease, what changes to crop diversity there will be, will irrigated area change). Changes to agricultural land are relative to the baseline (i.e. the year 2000), according to LUH2 and FAO data.
2. Calculate the future agricultural land, livestock area and maize cropping area based on these conditions. Current protected areas and future urban land are not included as potential future agricultural land.
3. An R function is used to calculate the national scale production associated with the cropping pattern. This function is then optimised to decide what is grown where in the future. The function is optimised using the R package Rsolnp (Ghalanos and Theussl, 2015) to return the maximum production given the prescribed area conditions and yield projections. This package optimises the function for crop production given various inequality and equality constraints – i.e. given that the overall crop area must equal x and that the maize area must equal y, and that each grid cell must not contain crop area greater than the available land specified at that grid cell, optimise the available land (i.e. optimise what is grown where in the available land) so that the cropping pattern with the most production is returned.
4. For futures with increasing crop diversity, arable area was diversified as much as possible given the arable area available (unless otherwise specified by stakeholders). This is achieved using a parameter that sets the maximum fraction of crop area that can be allocated to any one crop, which is reduced as much as possible (to 4 decimal places) to minimise the area allocated to any one crop, i.e. maximising

crop diversity in the optimisation function. For example, in the baseline in Zambia, the top 18 crops in terms of growing area use up more than 99% of arable crop land. In the future following optimisation with increased crop diversity, 25 crops use up 99% of arable crop area.

5. For futures with crop diversity decreasing, the percentage increase in the number of crops required to use up 99% of crop area for the crop diverse futures is reciprocated, so an equal decrease in crop diversity is simulated. For example, instead of the 7 crop increase described above for Zambia (18 to 25 crops), a 7 crop decrease is simulated, going from 18 crops in the baselinet to 11 in the future. This is achieved by setting the same parameter to the lowest value (at 4 decimal places) that achieves 99% of crop area for the required number of crops.
6. Lastly decide where the required pasture for livestock is placed in the remaining available land following crop area placement. Firstly place pasture in grid cells where the most pasture is in future, as defined in the LUH2 dataset. Then place pasture in any other available land.

For the future scenarios where land use was not optimised (i.e. the land use methods for "low tech" futures):

- The optimiser is not used for the low tech / low market connectivity / ineffective policy futures, and is also not used for any South African scenarios (as technology was not clearly associated with any scenario axis in South Africa).
- For these futures, a simpler approach is taken, where crops are by default kept in the same proportion as the baseline and simple changes to area in each grid cell are applied. For example, a 10% increase to all arable crop area in each grid cell if a 10% arable area expansion is required.
- If there are any changes to crop diversity for these futures, area is taken away from maize and evenly distributed to the other crops for increasing crop diversity, and area is evenly taken away from other crops and given to maize for the decreasing diversity futures.

Scenario assumptions for iFEED case study countries are as detailed in Table S5.

Land use and yield change assumptions:

- If arable area falls in a grid cell, this is allocated to grassland (checks are made to ensure enough grassland is available in future).
- All arable land increasing comes from grassland.
- Three grid cells for one crop in South Africa had 0 yield in baseline, resulting in infinite values for percentage change. For these grid cells the mean percentage change for this crop was used.
- The polygon data mapped by the WDPA team were used rather than reported areas as there were errors found in the reported statistics in the WDPA - e.g. in Malawi, a protected area was recorded as c. 800,000 ha whereas it should actually be c. 80,000 ha – this correction is made in the mapped data.

1.4 iFEED livestock production

1.4.1 Livestock regressions

- Herrero et al. (2013) have four categories of livestock feed: pasture, residues, grain-based and occasional. We will calculate changes to these food categories.
- Grains and occasional categories include all feed listed in FAOSTAT commodity balance sheets (Herrero et al., 2013).

- There are seven livestock production categories in Herrero et al. (2013) data that are used to train regressions: bvmeat (bovine meat), bvmilk (bovine milk), sgmeat (sheep and goat meat), sgmilk (sheep and goat milk), pimeat (pig meat), pomeat (poultry meat) and poeggs (poultry eggs).
- Many of the livestock food variables are correlated to each other, which can lead to multicollinearity in regressions – e.g. sometimes the sign of the relationship between the independent variables (feed sources) and the dependent variable (livestock production) changes from positive to negative when adding all of the independent variables compared to just one or two (in spite of positive correlations between the predictors and livestock production).
- To avoid multicollinearity in regressions, the livestock feed categories were aggregated by adding feed source variables together. The grains and occasional categories were combined as one variable (i.e. all feed from crop production and supplemental feeds such as groundnut hay in one variable) and the pasture and residues were combined to form a second variable (the pasture and residue variables across livestock products and countries showed the highest number of significant correlations from all combinations of two independent variables – i.e. the most collinearity).
- This results in a higher quality livestock feed variable (the crop production / occasional food supplements variable) and a lower quality feed variable (residues and pasture) and avoids unrealistic relationships emerging between feed sources and livestock production variables due to collinearity.
- Omit predictor variables from the regressions if the correlation between the predictor and the livestock production variable is insignificant. This is the case with Malawi sgmilk with both aggregated feed variables, and Zambia sgmilk for the crop production variable.
- In the case of Malawi sgmilk, as no predictor variables had significant correlations between livestock production and livestock food variables, we use coefficients calculated using data for all countries for sgmilk.
- Calculate national level regressions based on the aggregated predictor variables and the production data at every grid cell.
- If there are still any changes of sign in coefficients due to collinearity in regression variables, aggregate the feed variables again (resulting in one livestock food predictor variable used). This only happens with the pasture and residuals variable for the South Africa sgmeat regression, where a marginal negative coefficient is found when including both variables. In this case, one aggregated feed predictor variable is used.

1.4.2 Linking regressions to livestock commodities for emissions and production changes

The following percentage changes are applied to both FBS production data and to FAOSTAT emissions data.

For emissions:

- Apply the relevant percentage change for each livestock category, as listed below
- For sheep and goats, FAOSTAT data do not disaggregate between dairy and non-dairy herds, therefore calculating a percentage change for total across milk and meat herds by adding up base and future values for all sheep and goats.

Will not change the following as Herrero data do not cover these livestock categories: Meat, other – consisting of: Default composition: 1089 Meat, bird nes, 1097 Meat, horse, 1108 Meat, ass, 1111 Meat,

mule, 1127 Meat, camel, 1141 Meat, rabbit, 1151 Meat, other rodents, 1158 Meat, other camelids, 1163 Meat, game, 1164 Meat, dried nes, 1166 Meat, nes, 1172 Meat, nes, preparations, 1176 Snails, not sea

For the following commodities, apply percentage changes calculated using regressions directly:

1. Pigs: Regression linking grain to pig meat production. FBS commodities changed based on projected changes to pig meat:

- Pigmeat: Default composition: 1035 Meat, pig, 1038 Meat, pork, 1039 Bacon and ham, 1041 Meat, pig sausages, 1042 Meat, pig, preparations

2. Poultry: Regressions linking grain to eggs and meat production. FBS Commodities changed based on projected changes to poultry meat / poultry eggs:

- - Poultry meat: Default composition: 1058 Meat, chicken, 1060 Fat, liver prepared (foie gras), 1061 Meat, chicken, canned, 1069 Meat, duck, 1073 Meat, goose and guinea fowl, 1080 Meat, turkey
- Eggs

3. Sheep and goats: Mutton and goat meat, Default composition: 977 Meat, sheep, 1017 Meat, goat

4. Bovine meat, Default composition: 867 Meat, cattle, 870 Meat, cattle, boneless (beef and veal), 872 Meat, beef, dried, salted, smoked, 873 Meat, extracts, 874 Meat, beef and veal sausages, 875 Meat, beef, preparations, 876 Meat, beef, canned, 877 Meat, homogenized preparations, 947 Meat, buffalo Note that there are no buffalo according to FAOSTAT in AFRICAP countries, so bovine category = cattle / beef. Assuming cream changes in proportion with bovine milk change.

The following are the aggregated FBS livestock commodities:

For the following aggregated livestock production categories in the FBS we add up the relevant mean grid cell level data that the regressions are based on in the baseline and future and calculate a combined percentage change for each aggregated category.

1. Aggregate all meat categories (sgmeat, bvmeat, pomeat, pimeat) for Offals, edible and for Fats, Animals, raw: - Offals, edible, Default composition: 868 Offals, edible, cattle, 878 Liver prep., 948 Offals, edible, buffaloes, 978 Offals, sheep,edible, 1018 Offals, edible, goats, 1036 Offals, pigs, edible, 1059 Offals, liver chicken, 1074 Offals, liver geese, 1075 Offals, liver duck, 1081 Offals, liver turkeys, 1098 Offals, horses, 1128 Offals, edible, camels, 1159 Offals, other camelids, 1167 Offals, nes

2. Fats, Animals, raw, Default composition: 869 Fat, cattle, 871 Fat, cattle butcher, 949 Fat, buffaloes, 979 Fat, sheep, 994 Grease incl. lanolin wool, 1019 Fat, goats, 1037 Fat, pigs, 1040 Fat, pig butcher, 1043 Lard, 1065 Fat, poultry, 1066 Fat, poultry, rendered, 1129 Fat, camels, 1160 Fat, other camelids, 1168 Oils, fats of animal nes, 1221 Lard stearine oil, 1222 Degras, 1225 Tallow, 1243 Fat, nes, prepared

3. Aggregate svmilk and bvmilk for Milk, Excluding Butter and for Butter, ghee: - Milk, Excluding Butter, Default composition: 882 Milk, whole fresh cow, 888 Milk, skimmed cow, 889 Milk, whole condensed, 890 Whey, condensed, 891 Yoghurt, 892 Yoghurt, concentrated or not, 893 Buttermilk, curdled, acidified milk, 894 Milk, whole evaporated, 895 Milk, skimmed evaporated, 896 Milk, skimmed condensed, 897 Milk, whole dried, 898 Milk, skimmed dried, 899 Milk, dry buttermilk, 900 Whey, dry, 901 Cheese, whole cow milk, 903 Whey, fresh, 904 Cheese, skimmed cow milk, 905 Whey, cheese, 907 Cheese, processed, 908 Milk, reconstituted, 909 Milk, products of natural constituents nes, 910 Ice cream and edible ice, 917 Casein, 951 Milk, whole fresh buffalo, 954 Milk, skimmed buffalo, 955 Cheese, buffalo milk, 982 Milk, whole fresh sheep, 984 Cheese, sheep milk, 985 Milk, skimmed sheep, 1020 Milk, whole fresh goat, 1021

Cheese of goat mlk, 1023 Milk, skimmed goat, 1130 Milk, whole fresh camel - Butter, ghee, Default composition: 886 Butter, cow milk, 887 Ghee, butteroil of cow milk, 952 Butter, buffalo milk, 953 Ghee, of buffalo milk, 983 Butter and ghee, sheep milk, 1022 Butter of goat mlk

1.5 iFEED climate model subset used in ECOSSE modelling and trade and nutrition analysis

A subset of climate models is used for the nutrition and trade analysis and ECOSSE simulations due to large processing requirements (human and computational requirements are high for the two analyses respectively) and a lack of sensitivity in modelled outcomes to climate model inputs.

Methods used to select this subset are based on those of Ruane and McDermid (2017). This splits the models into 5 groups: Hot wet, Hot dry, Cold wet, Cold dry and Middle. It then picks a representative model from each category by calculating mean precipitation and temperature changes and selecting the model that is closest to these mean changes.

The subset was based on rainy season rainfall and temperature change, RCP8.5, over a region that includes all four iFEED countries. Note that the naming for the categories is relative to the ensemble change - a model classified as Cold wet for Regional, is cold and wet relative to the rest of the ensemble, but projects a future that is warmer and with a shorter rainy season than the present day.

All 29 models of Famien et al. (2018) are included in the subsetting process to select models that were representative of the range in the full ensemble, rather than just the 18 models used in the iFEED food production analysis.

ACCESS1-0 was the representative model for the 'mid' category, but was replaced with GFDL-CM3 as it is not included in the 18 model iFEED ensemble. The subset was based on RCP8.5 as this RCP is associated with larger climatic changes and one subset was required across both RCPs. Therefore, the subset based on rainfall and temperature, over the entire region of interest, using RCP8.5, was as follows: bcc-csm1-1-m (Cold dry) MRI-CGCM3 (Cold wet) MIROC-ESM-CHEM (Hot dry) IPSL-CM5A-LR (Hot wet) GFDL-CM3 (Mid; replacing ACCESS1-0)

1.6 iFEED trade and nutrition analysis supplementary methods

The trade and nutrition analysis uses data on food supply (from domestic production, international trade, and FAO Food Balance Sheet data), nutritional content of foods, and population level nutritional requirements in order to calculate nutrition security outcomes. This section contains more information on the data inputted to the analysis.

1.6.1 Food supply

For each country, the analysis brings together three datasets to derive the 2050 food supply:

1. FAO Food Balance Sheets (FBS) for baseline years 1998-2002. These quantify the mass of food supply per food item, broken down as shown in Table S6. Processing, feed, seed, and other uses are all assumed to account for the same proportion of the domestic supply quantity as they do in the baseline period. Avoidable household waste accounts for the same proportion of food as in the baseline period. Non-food uses are in the same proportions to domestic supply as in baseline year

2. Crop models and derivations covering all the crop related food in the FBS food items, expressing the percentage change in the mass of domestic food item production between the baseline period 2000 (1990 to 2010) and 2050 (2040 to 2060). 2050 values vary by scenario quadrant. For food items that are

extracted or otherwise processed from other primary commodities, 2050 production volumes are calculated based on the modelled production volumes of the primary commodity and country-specific 2013 extraction rates provided in FAO Supply Utilization Accounts. For the few food items where no 2050 production or extraction volumes were calculated, production volumes were kept constant at baseline values (e.g. seafood).

3. Mass quantifications of food items imported and exported in 2050 under four distinct trade vignettes:

a. Self sufficiency: Depicts a situation with no imports or exports, demonstrating the extent to which domestic production can meet population level nutritional requirements if international trade is eliminated; which nutrients have the largest production deficiencies given domestic requirements; which, if any, nutrient surpluses are available for export without impinging on population-level nutrient security.

b. Business as usual: Proportionally, baseline patterns of trade and domestic supply are unchanged, to illustrate how well current trading relationships may stand up to future needs to achieve nutrition security at a country level; how much proactive effort is required to increase (domestic/imported) supplies of certain nutrients.

c. Stakeholder expectations: A taskforce of in-country experts was asked to signal expectations about 2050 import and export dynamics for each scenario quadrant. Their increase/decrease/no-change expectations were quantified unilaterally by the core iFEED team across all food items relative to business-as-usual proportions. These are adjustable in aggregate or on a per commodity basis if preferred. e.g. BAU: 20% of an item produced in-country is exported. 50% increase under stakeholder expectations = 30% of item's production is exported.

d. Trade optimisation to achieve population level nutrition security using a linear optimisation approach to create an example of the food supply needed for nutrition security. This achieves population-level nutrition requirements (see below) by making the smallest possible changes to current food supplies and by being culturally sensitive to national dietary patterns, and indicates potential trade dependencies required to achieve nutrition security based on this food supply given domestic production outcomes.

The linear optimisation does not contain any intrinsic assumptions about trade, neither imports or exports. Rather, the optimisation is performed with reference to the total food supply; it is agnostic to where this supply is sourced from and assumes that no extrinsic sourcing constraints exist. Once the supply has been optimised, 2050 domestic production volumes (from the crop models) are accounted for and import and export volumes are calculated to balance the overall supply. Thus, for each food item, imports equate to the shortfall between optimised supply and domestic production and exports equate to the surplus domestic production volumes over and above the optimised requirements, and which are therefore available to trade. The specific constraints applied to the linear programming were to achieve nutrition security and to minimise deviation from the diet (baseline 1998-2000):

- The aggregate food supply was required to equal the population's average dietary energy requirements. For all nutrients, the returned per capita supply had to match or exceed the RNI and could not exceed the maximum thresholds for fats (see below).
- For all food items, the supply could increase to the maximum supply per capita in any country globally in 2013 (the latest available year in the FAO data at the time of the study rather than baseline years, since the exercise is forward looking).
- For alcohol, spices, tea, coffee or infant food, no increases were permitted above baseline amounts (to keep the supply quantities realistic)

- For offal, no increase was permitted above baseline amounts to keep the amount in the supply realistic and disproportionate to supply of other meat from livestock.
- For palm kernels, no increases were permitted since they are rarely used for human consumption.
- New food items not supplied to the country in the baseline period could be introduced up to the maximum supply per capita in any country globally based on 2013 FAO data.
- For milk and dairy products, any increases were limited to 110 grams per capita because the increase in some countries was viewed by the researchers as unrealistically high to achieve and it would disproportionately dominate the diet.
- For all food items, the supply could decrease by 50 per cent relative to the supply in the baseline period. If no solution was found then the supply could be decreased further in 5 per cent steps.

Items excluded from the FBS analysis, or other relevant assumptions/notes:

- Malawi soybean area and production data are not available for the year 2000 but are for 2003. Therefore area data for 2003 are used. This is the only example of a crop that does not have area and production data for the year 2000, but has data at another point in the time series.
- Watermelons and melons, other (inc. cantaloupes) are listed as constituent crops for both ”Fruits, other” and ”Vegetables, other”. These are only including in ”Fruits, other” in production change calculations.
- For four commodities in Malawi, there is production data but no area data in 1990-2010 (and no FBS production data) so the following commodities are not included in the Malawi analysis: ”Lemons, limes and products”, ”Apples and products”, ”Oranges, Mandarines”, ”Sweet potatoes”. Also Malawi has no roots and tuber nes area data, although it has production data that almost matches the FBS production data. But as there is no area data for any of the constituent crops in ”Roots, other” production changes for this category are not included. Tung nuts were excluded as they are toxic and so not eaten (and therefore no Oilcrops, other production projections are provided for Malawi, as tung nuts were the only constituent crop for this category in Malawi).
- Note that for sweet potato in Malawi, we are assuming that the potato production and area data include sweet potato (based on the breakdown of numbers in 2013:2014). Therefore, sweet potato nutrients are accounted for in the analyis, by assuming potato production breaks down into potato and sweet potato production.
- Malawi pineapple has no data in the FBS but there is growing area according to FAOSTAT. We therefore include Malawi pineapple production changes in the ”Fruits, other” category.
- There is South Africa FBS production data for ”Sweeteners, other” but not for the only constituent crop (sugar crops nes) so production changes for ”Sweeteners, other” were not included in the analysis.
- In South Africa, there is ”Rape and Mustardseed” production data in 2002 in FBS but not before. There is crop production data for rapeseed in the crop section for 1992 onwards however. Production changes are therefore calculated for this commodity, but there is only one year of data in the baseline period in the analysis in South Africa.

1.6.2 Nutrient content of foods

The nutrient values were calculated for each of the 96 aggregated food commodity groups in the FBS. First, these groups were disaggregated into the food items in the groups (as per the FAO FBS handbook). The food items were then matched to individual foods in food composition tables (FCT) providing the nutrient values per 100g. Country specific FCT were used for South Africa and Tanzania, and in the

absence of country specific FCT for Malawi and Zambia, the West African composition tables were used since these are the closest match. If a food item was not in these FCT then data would be taken from the US Department of Agriculture (USDA) FCT and then McCance and Widdowson (UK) FCT. This is a standard methodology. The nutrients included are total fat, saturated fat, protein, carbohydrate, fibre (AOAC), vitamin A (RAE), vitamin B (thiamine, riboflavin, niacin, B6, folate), vitamin C, calcium, iron and zinc, as well as energy. Unfortified forms of foods were taken from the FCT, except in the case of flour and maize in South Africa where legislation determines these are fortified.

- Assumes the same nutrient profiles for imports as domestic production.
- Assumes no change in nutrient densities between baseline (publication dates for the FCT) and 2050 (including no change with increases of atmospheric CO_2)
- Wheat flour is assumed to be wholegrain unless food consumption surveys indicate otherwise.
- Assuming white maize is the maize that is fed to people in the FBS.
- The weighting of certain food items within a commodity which vary significantly in a key nutrient (e.g. the commodities sweet potato, palm oil and offal have varieties varying widely in vitamin A) is based on consumption data where possible, otherwise data from other sources (e.g. industry data) informed the calculations. Expert opinion would be taken on types of food eaten, e.g. what offal is consumed, but in some cases it was not possible to quantify the amount consumed and an unweighted average would be used.

Before the food items were aggregated back to the food commodity groups in the FBS each food item in a group was weighted to reflect the consumption of those foods within each country. A weighted average was then calculated and used in the estimated nutrient profile of the commoditiy groups. This avoided an over- or underestimate of nutrient content at a group level. At the time of the study the weightings used by the FAO were not publicly available. Data we used for the weighting came from household food surveys (Malawi and South Africa) but these do not exist in Zambia or Tanzania, so the household food expenditure survey and household budget survey were used, respectively.

The calculated supply values (daily per capita) were plotted against those nutrients reported in the FBS (energy, fat and protein). Any mismatches / outliers for a food item were identified and investigated. If there was no error in the food composition values, these values were taken to be correct for that country. The FAO methodology for estimating energy, fat and protein is not published therefore it is unknown how they calculate these values or FCT they use. However, the AFRICAP calculated values were very closely matched to the FAO values in the FBS. Example comparisons are shown in Figures S7 to S9.

All the food groups were adjusted for unavoidable waste (e.g. bones, inedible peel) to represent only the food consumed. Data were taken from the USDA FCT.

The product of the unitary nutrient contents of each food item and the supply of the respective food item provides the total nutrient supply per food commodity group and across the entire food balance sheet. To assess the adequacy of the nutrients supplied (after accounting for non-food uses, losses and household waste) requires insights about the population's requirements.

1.6.3 Population-level energy and nutrient requirements

On a per capita basis, population-level energy and nutrient requirements vary depending on the sex and age of individuals, with pregnancy-specific requirements for reproductive-age females. These population-level per capita nutrient requirements were specific to the population demographics in each of the four AFRICAP

countries. The reference values were taken from the World Health Organization dietary recommendations (2004). The nutrients included for this project are total fat, saturated fat, protein, carbohydrate, fibre (AOAC), vitamin A (RAE), vitamin B (thiamine, riboflavin, niacin, B6, folate), vitamin C, calcium, iron, zinc.

For the majority of nutrients, adequacy is based on three threshold values: Reference Nutrient Intake (RNI), Estimated Average Requirement (EAR), and Lower Reference Nutrient Intake (LRNI). The RNI is the principal target representing a level of nutrient intakes that are adequate for 95 per cent of the population. The EAR is an intake adequate for half the population, and the LRNI is a lower-bound target representing an adequate nutrient intake for 2.75 per cent of the population. For saturated fat, total fat, and energy supply, different thresholds apply. Fat and saturated fat targets are expressed as ranges proportional to the energy supply quantity. In both cases if the minimum energy supply target is satisfied, this is proportional to actual supply; if the minimum energy supply target is not satisfied, this is proportional to target supply. Saturated fat has no minimum requirement; the maximum recommendation is 10 per cent of the total energy supply. For total fat, the recommended intake is in the range of 15 to 30 per cent of total energy intake. Energy requirement thresholds are the minimum, average (principal), and maximum dietary energy requirements (MDER, ADER, XDER) (see Naiken, 2014).

RNI used for zinc and iron assumes low bioavailability values (5% iron and 15% zinc) since the diets in the iFEED countries are typically high in plant-based foods where bioavailability of these nutrients is low compared to animal products.

Per capita requirements are scaled-up to aggregate population requirements based on annual demographic data for each country, stratifying expected population numbers by sex and 5 years age bracket and estimating age-specific fertility rates (births per 1000 women). These demographic data are obtained from the medium fertility estimates in the UN DESA Population Division's World Population Prospects 2019.

With these components, the population-level supply of each nutrient can be assessed relative to the population's requirements, as the marker of nutrition security.

1.7 GLAM crop model parameterisation and evaluation

1.7.1 Input data

The EWEMBI data set (Lange, 2019) was used as the climate input data for crop model evaluation in the historical period. The EWEMBI data set was compiled for bias-correction of climate input data for the Inter-Sectoral Impact Model Intercomparison Project (ISI-MIP; Frieler et al., 2017).

The EWEMBI data cover the globe at 0.5 degree spatial and daily temporal resolution from 1979 to 2013. Data sources of EWEMBI are ERA-Interim reanalysis data (ERAI; Dee et al., 2011), WATCH forcing data methodology applied to ERA-Interim reanalysis data (WFDEI; Weedon et al., 2014), eartH2Observe forcing data (E2OBS; Calton, 2016) and NASA/GEWEX Surface Radiation Budget data (SRB; Stackhouse, 2011). SRB data were used to bias-correct E2OBS shortwave and longwave radiation (Lange, 2018).

Grid cells are selected for evaluation simulation if they contain maize growing area, as defined by MIRCA (Monthly Irrigated and Rainfed Crop Areas – Portmann et al., 2010), representing information from the years 1998-2002. Irrigation is determined by a majority grid cell approach. If a grid cell contains greater than 50% of growing area irrigated, supplementary irrigation simulations are used for that grid cell. This irrigation routine provides as much as 1 cm of irrigation water to the crop if soil water falls below a fraction of available soil water. Otherwise simulations for the grid cell are rainfed. For the four modelled crops

of maize, groundnut, potato and soybean, no grid cells in Malawi and Zambia had greater than 50% of growing area irrigated for any crops, whereas 1 in Tanzania and 13 in South Africa did for maize. South Africa also had 10 and 12 grid cells irrigated for potato and groundnut respectively, which were mostly a subset of the same grid cells irrigated for maize. No grid cells were irrigated for soybean.

Simulations were used to assess if there were any significant differences between irrigated simultions using the majoritiy grid cell approach and a more computationally-intensive weighted mean approach, where both rainfed and irrigated simulations are conducted and the proportion of irrigated area is represented by the irrigated simulations, and the proportion of rainfed by rainfed simulations. These results were virtually identical in South Africa and Zambia where the model was tested with the weighted mean approach. Therefore the majority grid cell approach was favoured as it requiredsfewer simulations. See Figures S1 and S2 for outputs using the two methods in South Africa - the country with most irrigation out of the four AFRICAP countries.

There are differences in the crop data sets available to modellers (Porwollik et al., 2017). However, most differences occur in crop areas with a smaller amount of growing area, and in Eastern and Southern Africa in particular available data sets are relatively similar (Anderson et al., 2015). Uncertainty due to growing area data sets is therefore assumed to be relatively small.

1.7.2 Crop model parameterisation and configuration

Table S1 to S4 in list all crop-specific parameter values (and ranges where applicable) for GLAM used in this analysis. For maize, parameters are mainly based on those previously used by Asfaw et al. (2018), and thermal time ranges are from Durand et al. (2017). Parameters are largely based on Osborne et al. (2013) for soybean, Challinor et al. (2004) for groundnut, and Jennings et al. (2020) for potato.

Parameters were checked to ensure that they simulate realistic potential rainfed yields (according to the Global Yield Gap Atlas - e.g. see van Bussel et al., 2015) when the yield gap parameter C_{YG} was set to 1 (meaning that yields for the region should be at climatic potential rainfed yields).

Initial model simulations are used to assess model skill in the historical period of 1980 to 2009. For these simulations, the 15 year time series within this period with the strongest correlation between observed yields and crop area weighted weather variables was used to evaluate the model, with other available data used to calibrate the model. This is because some sections of the observed yield time series have extremely poor correlations with weather variables and therefore there is very little signal for the model to compare to. The section of the time series with the most significant correlations was chosen for model evaluation; the other half of the baseline period is used for model calibration and the selection of planting windows and variety parameters. Planting dates and varieties are selected using the full time series of data for these initial simulations. C_{YG} is then calibrated on the full time series. Each 15 year time series starting from 1980 to 1995 is then evaluated to assess which has the strongest correlation with weather variables. In particular, sections of the time series with significant correlations between rain/temperature and yields are sought. The time series with the most significant correlations is selected for evaluation - preferably, with both temperature and rainfall correlations being significant at the P-value of 0.05 level; failing that, at the 0.1 level. If none of these significant correlations are found, the first half of the time series is used for calibration, and the second half is used for evaluation.

Following selection of years for model calibration and evaluation, calibration years are used to firstly select the planting dates and crop varieties at each grid cell. Possible planting windows are selected from FAO crop calendars and in some cases personal communications from project partners. Different crop

varieties – representative of current short, medium and long-maturing varieties – are also tested. The combination of variety and planting window that results in the highest simulated yield is selected at each grid cell, providing emergency planting (i.e. planting at the end of the planting window) does not take place for a majority of years in the time series and that durations are within realistic bounds (taken to be less than 200 days for most crops; for potato and groundnut this is less than 180 days as growing seasons are typically shorter for these crops).

Planting date and variety selection simulations for future climate were carried out on all years from 1990 to 2088 using a 20 year rolling mean approach (coinciding with time slices used for baseline and future in the analysis, as well as the typical period over which breeding takes place in sub-Saharan Africa - Challinor et al., 2016), with YGP set to 1 and irrigation assumed the same as the baseline (the irrigation routine provided as much as 1 cm of irrigation water to the crop if soil water fell below a fraction of available soil water. For future climate, for areas where irrigation was expanded to those areas not irrigated in the baseline, we irrigated by a maximum of 1 mm per day if soil water falls below a specified soil moisture threshold. This amount was agreed in conjunction waith stakeholders). Therefore planting dates and varieties were selected for each year, from baseline to future, but not for each YGP or irrigation level. This is because firstly varietal choices and sowing window selection are independent of mean yields (i.e. not varying with YGP) and secondly that the selection of planting dates is based on current irrigation conditions, rather than for different possible irrigation levels that could potentially be used in future. Future planting dates used rainfed limitations applied where applicable, the assumption being that farmers will continue to be water efficient where possible.

A full range of C_{YG} options from 0.1 and 1 and irrigation levels were also simulated, providing a "look-up table" of simulations for the four crops modelled and various adaptation options. IRRSUPFRAC of 0.5 and 1 with MAXSUP 1 both lead to potential transpiration being achieved in South Africa and Zambia in the baseline. Therefore only two IRRSUPFRACs were simulated for look-up table simulations - 0.1 and 1 - with a variety of MAXSUP levels, to simulate the full extent of possible irrigation levels between potential yields and rainfed yields.

1.7.2.1 CO_2 fertilisation parameterisation

To take into account CO_2 fertilisation, GLAM is parameterised to match yield responses as recorded by Free Air CO_2 Enrichment (FACE) (Kimball, 2016). These FACE responses are representative of a 353 ppm concentration in the baseline (c. year 1988) and a 550 ppm concentration of CO_2 in the future - the equivalent of year 2053 for RCP8.5. In elevated CO_2 conditions, maize shows yield increases of 21 to 39% in water stressed conditions according to these data, and -4 to 0% change in ample water conditions. Potato has yield increases of 22 to 32%, soybean has a yield increase from -9 to 24% and groundnut has a 13 to 19 % increase. Typically transpiration reduces in elevated CO_2 conditions.

Simulations are conducted for years 1983 to 1993 (centred on 1988). GLAM parameters concerned with biomass growth (radiation use efficiency RUE, transpiration efficiency TE and the maximum normalised transpiration efficiency TENMAX) are increased incrementally, and the physiologically-limited potential transpiration PTM is decreased, ensuring that reductions in transpiration are driven by physiological (stomatal closure) and not energetic limitations (Challinor and Wheeler, 2008; Challinor et al., 2005). The combination of parameters that best matched FACE yield response ratios and achieve a decrease in transpiration to match FACE data are chosen for each crop (averaging across all grid cells included in the analysis). This process gives a parameterisation to capture a sensible yield response to elevated CO_2. The

baseline and these altered parameters are then interpolated and extrapolated to capture responses across a full range of CO_2 values.

Grid cells are selected for the CO_2 analysis that contain more than median growing area for that crop and are rainfed, and have durations greater than 100 days and yields greater than 0. From the cells that fulfil these conditions, simulations are conducted in Zambia (which has relatively high rainfall for the region) and South Africa (relatively low rainfall) that vary parameters to see which combination of best replicates the response ratios of Kimball (2016). Tests are focussed on these two countries as they most often display stronger correlations between observed yields and climate inputs and have resultingly high model skill in evaluation simualtions. Different rainfall conditions are included because we expect a different CO2 response in wet and dry conditions for C4 crops in particula (in this case, for maize). For Zambia, grid cells with greater than median rainfall are selected. For South Africa, grid cells with and without water stress are included (defined when the ratio of transpiration to potential transpiration falls below a crop-specific critical value, and median rainfall).

Pick the parameter combination that best fulfils mean yield response ratios, disregarding those that see yield decreases on average. Prioritise yield response first on average, then if possible have parameters so that wet condition response is lower than dry condition response for c4 crops and any c3 crops that have evidence of this such as soybean (i.e. zambia is wet, vs wet in safrica, vs dry in safrica). I am using the below Kimball paper for the response ratios. The Long 2006 paper gives the changing response ratios over time – if you are looking at a time slice this is of less interest.

For maize, only TE is increased as increasing RUE and TENMAX would result in larger yield increases in well-watered condtiions. Mean response ratios were best fulfilled for a 14% increase to TE and a 6% decrease in PTRANSMAX. This combination gave the smallest increase for wet conditions in South Africa whilst fulfiiling dry condition response ratios. This resulted in an average yield increase of 21% in South Africa, with response ratios within FACE bounds in dry conditions but slightly high in wet conditions (although still lower than dry response). Zambia average response was also lower than the South Africa dry conditions, although the national mean yield increase was slightly high for well-watered conditions at 20%.

For soybean, a 24% increase in TE, RUE and TENMAX and a 20% decrease in PTRANSMAX was the best parameter combination for fulfilling conditions for both countries. This fulfils mean Zambian and South African yield response ratios (yields progressively lower for South African wet and Zambian wetter conditions, and not changing for Zambia wet conditions). The mean yield response ratio is South Africa was a 21% increase. For Zambia, there was no yield change on average. Transpiration decreases slightly too much in zambia, but is within the response ratios in South Africa.

For potato, no parameter combination fulfilled all conditions for transpiration and yield. Therefore choosing from those that did so in Zambia and showed the largest yield in crease in South Africa whilst showing a reduction in transpiration. This was an increase of 6% and a decrease of 2%. The mean South African response ratio was a 14% increase, and in Zambia it was a 25% increase.

For groundnut, no parameter combination fulfils all conditions for transpiration and yield. Parameter comboination of a 10% increase and a 2% decrease was best. This fulfils South African and Zambian mean yield response ratios (being a 14 and 17% increase respectively).

Interpolation is then used to capture a sensible parameter response to the full range of possible CO_2 concentrations. Firstly, parameters varied to capture the CO_2 response (TE, RUE, TENMAX and PTRANSMAX) are interpolated between ambient and 550ppm values using linear interpolation. The data from Long et al. (2006) and Kimball (2016) suggest saturation of the CO_2 response at approximately 900

ppm. For C4 crops, approximately half the yield response to elevated CO_2 happens post-550 ppm according to the data of Long et al. (2006), and therefore half the response gradient is assumed for concentrations from 550-900ppm compared to ambient CO_2 to 550ppm. For C3 crops, a quarter of the gradient in relationships post-550ppm is shown according to the data of Long et al. (2006). Linear interpolation is then again used to ascertain parameter values for CO_2 concentrations between 550 and 900ppm.

1.7.3 Model evaluation results

1.7.3.1 Model evaluation - maize

For Malawi, 1983 to 1997 had the strongest correlation between observed yields and rainfall (p-value $<$ 0.05) so was selected for model evaluation (there being no significant correlations with temperature). 1998 to 2009 was used for calibration.

For Zambia, 1980 to 1994 and 1981 to 1995 had the strongest correlations between observed yields and rainfall (p-value $<$ 0.05). 1980 to 1994 had a slightly stronger correlation with temperature, so was selected for model evaluation (there being no significant correlations with temperature). 1995 to 2009 was used for calibration.

For Tanzania, correlations were weak with none significant at the 0.05 p-value level. The strongest correlations were between rainfall and observed yields for 1980 to 1994 (p-value 0.1) and temperature and observed yields from 1994 to 2008 (p-value 0.1). Simulations are mainly driven by temperature in Tanzania during this period as there is typically sufficient rainfall, therefore 1994 to 2008 was chosen for model evaluation, and 1980 to 1993 for calibration.

For South Africa the strongest correlations were from 1988 to 2002 (both temperature and rainfall correlation p-values $<$ 0.01) so these years were used for evaluation. 1980 to 1987 were used for calibration.

When calibrating C_{YG} to observed yields, low values of C_{YG} were recorded, with all countries having 0.08 when calibrating on increments of 0.02 (apart from Tanzania which had a calibrated value of 0.06), meaning that yields are far from climatic potentials for the region. GYGA show water-limited potential yields for tanzania and zambia to be 5.96 (2-13 depending on climate zone) and 11.33 (6-19 depending on climate zone) t/ha respectively. When setting C_{YG} to 1 to simulate potential yields, mean values range from 7.7 to 14.1 t/ha for the four africap countries.

Maize evaluation results in significant correlation coefficients at the p-value level of 0.1 for countries with some significant correlations between observed yields and weather variables (South Africa, Malawi and Zambia). South Africa has by far the strongest relationships between observed yields and weather variables, and also by far the best correlation coefficient between simulated and observed yields. See Figures S3 to S6 for observed and simulated yields at the national scale in South Africa.

FAO crop calendars show maize planting taking place from (occasionally September) October to December in the four countries, depending on the rainy season. Evaluation simulations restrict planting windows to these dates. Harvest takes place in simulations typically around 150 days after sowing, again in line with FAO information, where growing seasons may last upwards of 180 days in places but more usually around 150 days.

1.7.3.2 Model evaluation - soybean

Malawi only has soybean yield data starting in the year 2003, and therefore was excluded from the interanual variability evaluation process. Tanzania had insiginficant relationships between observed yield and weather variables so was also excluded. The two countries with signifcant weather-observed

relationships also show significant correlations between observed and simulated yields - South Africa has a correlation of 0.54 (p-value < 0.05) and Zambia has a correlation of 0.64 (p-value < 0.01).

When calibrating C_{YG} to observed yields, higher values of C_{YG} were recorded which is expected given the smaller yield gap in the region for soybean (see GYGA). In Malawi C_{YG} is 0.58, in Tanzania it is 0.6, in South Africa it is 0.72 and in Zambia it is 0.78.

GYGA do not have soybean potential yield values for the AFRICAP countries, although there are values for Uruguay and Argentina of 3.2 and 3.9 t/ha respecitvaly, which are similar to the simulated mean potential yield in Malawi of 3.6 t/ha, with the other countries being slightly lower, typically around 2-2.5 t/ha.

Planting dates were similar to those simulated for maize - planting strongly being linked to the rainy season in the region. Growing season durations are typically slightly shorter for soybean - again in line with FAO crop calendar information.

1.7.3.3 Model evaluation - potato

Zambia and Tanzania potato yield data from FAOSTAT had virtually 0 interannual variability so were excluded from the model einteranual variability evaluation process. Malawi also has no signicant relationship between temperature and observed yields, and rainfall is not a limiting factor in terms of its relationship with observed yields (it having a negative correlation between rainfall and observed yields - i.e more rainfall, and therefore less solar raditation, leads to lower yields). Therefore only South Africa was assessed in terms of interannual variability. GLAM-potato is otherwise extensively evaluated against global observations in Jennings et al. 2020.

South Africa has insignifcant relationship between observed yields and rainfall, but a significant correlation with temperature that is well-captured in simulations. GLAM does less well at simulating the interannual variability of observed yield, with a correlation of 0.35 (p-value 0.2).

When calibrating C_{YG} to observed yields, in Tanzania C_{YG} is 0.05, in Malawi it is 0.08, in Zambia it is 0.1 and in South Africa it is 0.12.

GYGA do not have potato potential yield values for the AFRICAP countries, and only report data for China with rainfed potential yields of around 43 t/ha. Simulated mean potential yield values range from about 15 to 18 t/ha in the AFRICAP countries.

Planting ad harvest dates are similar to those of maize, with rainfall largely determining the growing season.

1.7.3.4 Model evaluation - groundnut

Malawi has a correlation between observed and simulated yields of 0.46 (p-value < 0.1). South Africa has a correlation of 0.47 (p-value < 0.1). Zambia, with particularly strong observed yield-weather variable correlations, also simulates inerannual variability of years extremely accurately with a correlation of 0.81 (p-value < 0.001). Tanzania has an insignificant correlation between observed yields and simulated yields, due to weaker relationships between observed yields and weather variables.

When calibrating C_{YG} to observed yields, in Tanzania C_{YG} is 0.22, in Malawi it is 0.22, in Zambia it is 0.18 and in South Africa it is 0.48.

GYGA have rainfed potential yield data for Tanzania of 2.3 t/ha. Simulated mean potential yield values range from about 1.6 to 3.6 t/ha in the AFRICAP countries.

Planting ad harvest dates are similar to those of maize, with rainfall largely determining the growing season.

1.8 Supplementary Tables and Figures

Table S1: Parameters used in GLAM-maize, with ranges where applicable.

Parameter	Explanation	Value (range)	Reference
Leaves			
DLDTMX	Maximum daily increase in LAI	0.15	Durand et al. (2017)
MASPA	Minimum daily increase in senesced LAI during leaf senescence.	0.05	Bergamaschi et al. (2013)
SWF_THRESH	Critical value of soil water stress factor for leaves	0.7	Bergamaschi et al. (2013)
NDSLA	Specific Leaf Area control	5 days	Challinor and Wheeler (2008)
SLA_INI	Specific leaf area control (see Challinor and Wheeler 2008)	350 cm2/g	Richner et al. (1996); Ashraf and Hafeez (2004)
MAX_ISTG_SLA	Max development stage for SLA control	2 (until flowering)	N/a
Evaporation and transpiration			
ALBEDO	Albedo	0.2	Challinor et al. (2004)
CRIT_LAI_T	LAI below which transpiration is physiologically limited	2.7 (0.6 to 2.7)	Al-Kaisi et al. (1989); Bergamaschi et al. (2013)
P_TRANS_MAX	Max value of potential transpiration	0.73 cm/day (0.2-0.73)	Al-Kaisi et al. (1989)
VPD_CTE	Used to calculate vapour pressure deficit	0.7 (0.42 to 0.98)	Tanner and Sinclair (1983)
VPD_REF	Used to calculate Priestly-Taylor coefficient	1 kPa (0.6-1.4)	Steiner et al. (1991)
SHF_CTE	Used to calculate soil heat flux	0.4	Choudhury et al. (1987)

EXTC	Extinction coefficient	0.5 (0.3-0.85)	Bergamaschi et al. (2013)
Soil and roots			
ASWS	Initial soil water (fraction of water holding capacity)	0.7	Watson et al. (2015)
NWBDAYS	Number of days water balance is run before start of planting window	30 days	N/a
NSL	Number of soil layers	25	Challinor et al. (2004)
ZSMAX	Maximum rooting depth	150 cm	Asfaw et al. (2018)
RKCTE	Used to calculate saturated hydraulic conductivity of the soil	75 cm/day	Suleiman and Ritchie (2001)
UPDIFC	Uptake diffusion coefficient	0.25 cm2/day (0.19 to 0.3)	Jamieson and Ewert (1999); Robertson and Fukai (1994)
EFV	Extraction front velocity	2 cm/day (1.66 to 3.3)	Dardanelli et al. (1997); Bergamaschi et al. (2013)
DLDLAI	Increase in root length density at surface with LAI	1 cm/cm3	Bergamaschi et al. (2013)
RLVEF	Root length density at the extraction front	0.3 cm/cm (0.1 to 0.6)	Watson et al. (2015)
Biomass and yield			
TE	Transpiration efficiency	8 Pa (5.35 and 10.5)	Asfaw et al. (2018); Walker (1986); Adamtey et al. (2010)
TENMAX	Max. normalised transpiration efficiency	11 g/kg	Walker (1986); Adamtey et al. (2010); Pilbeam et al. (1995)
RUE	Radiation Use Efficiency	3.5 (2-5) (g/MJ)	Kiniry et al. (1989); Lindquist et al. (2005)
DHDT	Maximum daily increase in harvest index	0.0085 (0.002-0.018	Durand et al. (2017)

MAX_HI_MAIZE	Maximum harvest index for maize	0.6	Hay and Gilbert (2001)
Development			
FSWSOW	Fractional soil moisture for intelligent planting and emergence	0.5	Challinor et al. (2004)
IEMDAY	Number of days from planting to emergence	6	Ashagre et al. (2001)
I_TTCALC	Shape of function to calculate thermal time	1 (flat top)	Keating et al. (1992)
TBMAI	Base temperature for maize	10C	Sanchez et al. (2014)
TOMAI	Optimum temperature for maize	30C	Sanchez et al. (2014)
TMMAI	Maximum temperature for maize	40C	Sanchez et al. (2014)
I_PHEN	Complex (I_PHEN=0) or simple (I_PHEN=1) simulation of phenology	0	N/a
TLIMJUV	Thermal time from planting to the end of the juvenile phase	(150-500 degree days)	Durand et al. (2017)
TLIMSIL	Thermal time from tassel initiation to silking	150-650 degree days	Durand et al. (2017); Asfaw et al. (2018)
TLIMPFL	Thermal time from silking to start of grain filling.	20-200 degree days	Durand et al. (2017)
TLIMGFP	Thermal time from start of grain filling to maturity	150-700 degree days	Durand et al. (2017)
PPSEN	Photoperiod sensitivity	0-0.75	Durand et al. (2017)
Optional processes			
TETRS	Switch for temperature dependence of TE and RUE	1 (on)	N/a

TETR1	Temperature above which TE and RUE begin linear reduction	35 C	Yang et al. (2004); Carberry et al. (1989)
TETR2	Temperature above which TE and RUE are zero	47 C	Yang et al. (2004); Carberry et al. (1989)
TETR3	Temperature below which TE and RUE are zero	7 C	Yang et al. (2004); Carberry et al. (1989)
TETR4	Temperature below which TE and RUE begin linear reduction	18 C	Yang et al. (2004); Carberry et al. (1989)
HTS	Switch for heat stress around flowering	2	N/a
TSETCRIT	Switch for high temperature stress around flowering	35	Gourdji et al. (2013)
TSETZERO	Switch for high temperature stress around flowering	45	Sanchez et al. (2014)
TDS	Switch for terminal drought stress (TDS)	1 (on)	N/a
HIMIN	Minimum harvest index for TDS to occur	0.25	Challinor et al. (2009)
SWCFAC	Fraction of water holding capacity below which TDS occurs	0.05	Challinor et al. (2009)
I_EMER	Switch for intelligent emergence	1 (on)	N/a
TRKILL	Switch for lethal temperature parameterisation	1 (on)	N/a
TRKILL1	Temperature below which crop fails	-1.8;	Sanchez et al. (2014)
TRKILL2	Temperature above which crop fails	46	Sanchez et al. (2014)
WS	Switch for water stress around flowering	2 (on)	N/a
SWFFTHR	SWFAC threshold for damage to flowers	0.2	Challinor et al. (2006)

TRLAI	Switch for temperature dependence of LAI growth	1 (on)	N/a
TRLAIB	Base temperature below which leaf growth does not occur	7.3 C	Sanchez et al. (2014)
TRLAIO	Optimum temperature for leaf growth	31.1 C	Sanchez et al. (2014)
TRLAIM	Maximum temperature for leaf growth	41.3 C	Sanchez et al. (2014)

Table S2: Parameters used in GLAM-potato, with ranges where applicable.

Parameter	Explanation	Value (range)	Reference
Leaves			
DLDTMX	Maximum daily increase in LAI	0.14	Hay and Porter (2006); Jones and Allen (1983); Allen and Scott (1980);
MASPA	Minimum daily increase in senesced LAI during leaf senescence.	0.14	Jennings et al. (2020)
SWF_THRESH	Critical value of soil water stress factor for leaves	0.6	Ejieji and Gowing (2000); Jefferies and Heilbronn (1991)
NDSLA	Specific Leaf Area control	5 days	Challinor and Wheeler (2008)
SLA_INI	Specific leaf area control (see Challinor and Wheeler ,2008)	500 cm2/g	Vos and Biemond (1992); Fasan and Haverkort (1991)
MAX_ISTG_SLA	Max development stage for SLA control	2	N/a
Evaporation and transpiration			
ALBEDO	Albedo	0.2	Challinor et al. (2004)

CRIT_LAI_T	LAI below which transpiration is physiologically limited	2.8	Tanner and Jury (1976)
P_TRANS_MAX	Max value of potential transpiration	1.25 cm/day	Campbell et al. (1976)
VPD_CTE	Used to calculate vapour pressure deficit	0.7 (0.42 to 0.98)	Tanner and Sinclair (1983)
VPD_REF	Used to calculate Priestly-Taylor coefficient	1 kPa (0.6-1.4)	Steiner et al. (1991)
SHF_CTE	Used to calculate soil heat flux	0.4	Choudhury et al. (1987)
EXTC	Extinction coefficient	0.55	Haverkort et al. (1991); Jongschaap and Booij (2004); Monteith and Unsworth (2007)
Soil and roots			
ASWS	Initial soil water (fraction of water holding capacity)	0.7	Watson et al. (2015)
NWBDAYS	Number of days water balance is run before start of planting window	30 days	N/a
NSL	Number of soil layers	25	Challinor et al. (2004)
ZSMAX	Maximum rooting depth	100 cm	Jennings et al. (2020)
RKCTE	Used to calculate saturated hydraulic conductivity of the soil	75 cm/day	Suleiman and Ritchie (2001)
UPDIFC	Uptake diffusion coefficient	0.175 cm2/day	Lesczynski and Tanner (1976)
EFV	Extraction front velocity	1.75 cm/day	Smit and Groenwold (2005)
DLDLAI	Increase in root length density at surface with LAI	3.25 cm/cm3	Iwama et al. (1993)

RLVEF	Root length density at the extraction front	0.575 cm/cm	Lesczynski and Tanner (1976); Stalham and Allen (2001); Parker et al. (1989)
Biomass and yield			
TE	Transpiration efficiency	6.525 Pa (2-11.05)	Jefferies (1993); Kaminski et al. (2015); Tanner (1981); Vos and Groenwold (1989)
TENMAX	Max. normalised transpiration efficiency (g/kg)	11.31 g/kg	Vos and Groenwold (1989)
RUE	Radiation Use Efficiency	2.7 (1.7-3.7) (g/MJ)	Zhou et al. (2016); Timlin et al. (2006); Khurana and McLaren (1982); Jefferies and MacKerron (1989)
DHDT	Maximum daily increase in harvest index	0.012	Moriondo et al. (2005)
MAX_HI_SPUD	Maximum value of harvest index	0.8	Moriondo et al. (2005)
Development			
GCPOEMER, GCPOTUBI, GCPOSENE, GCPOHARV	Thermal time requirements (°days; stages 1, 2, 3, 4)	100-400, 100-300, 200-500, 100-400	Streck et al. (2007); Paula et al. (2005); Jefferies and Mackerron (1987); Van Keulen and Stol (1995)
TBPO, TOPO, TMPO	Cardinal temperatures (°C), base, optimum, maximum	4, 18, 29 (0-8, 15-21, 25-33)	Manrique and Hodges (1989); Sands et al. (1979)
Critical photoperiod P_{crit} (hours)	10.7-13	Ewing and Wareing (1978); Streck et al. (2007)	
PPSEN	Photoperiod sensitivity P_s	0.0645	Streck et al. (2007)
CRITPP	Critical photoperiod P_{crit} (hours)	10.7-13	Ewing and Wareing (1978); Streck et al. (2007)

FSWSOW	Fractional soil moisture for intelligent planting and emergence	0.5	Challinor et al. (2004)
I_TTCALC	Shape of function to calculate thermal time	0 (triangular)	Keating et al. (1992)
Optional processes			
TETRS	Switch for temperature dependence of TE and RUE	-1 (off)	Jennings et al. (2020)
HTS	Switch for heat stress around tuber initiation	2	Jennings et al. (2020)
TSETCRIT	Switch for high temperature stress around tuber initiation	24	Timlin et al. (2006); Wolf et al. (1990); Ingram and McCloud (1984)
TSETZERO	Switch for high temperature stress around tuber initiation	33	Timlin et al. (2006); Wolf et al. (1990); Ingram and McCloud (1984)
TDS	Switch for terminal drought stress (TDS)	1 (on)	N/a
HIMIN	Minimum harvest index for TDS to occur	0.25	Challinor et al. (2009)
SWCFAC	Fraction of water holding capacity below which TDS occurs	0.05	Challinor et al. (2009)
I_EMER	Switch for intelligent emergence	-1 (off)	N/a
TRKILL	Switch for lethal temperature parameterisation	1 (on)	N/a
TRKILL1	Temperature below which crop fails	-2;	Sanchez et al. (2014)
TRKILL2	Temperature above which crop fails	46	Sanchez et al. (2014)
WS	Switch for water stress around flowering	0 (off)	Jennings et al. (2020)

TRLAI	Switch for temperature dependence of LAI growth	-1 (off)	Jennings et al. (2020)
HTSEN_SWITCH	Switch for tincreased senescence with high temperatures	1 (on)	Jennings et al. (2020)
HTS_SEN	Threshold when exceeded by TMAX there is an increase in leaf senescence (degrees C)	34	Raymundo et al. (2017)

Table S3: Parameters used in GLAM-groudnut, with ranges where applicable.

Parameter	Explanation	Value (range)	Reference
Leaves			
DLDTMX	Maximum daily increase in LAI	0.1	Challinor et al. (2004)
SWF_THRESH	Critical value of soil water stress factor for leaves	0.7	Challinor et al. (2004)
NDSLA	Specific Leaf Area control	5 days	Challinor and Wheeler (2008)
SLA_INI	Specific leaf area control (see Challinor and Wheeler 2008)	300 cm2/g	Challinor and Wheeler (2008)
MAX_ISTG_SLA	Max development stage for SLA control	2	N/a
Evaporation and transpiration			
ALBEDO	Albedo	0.2	Challinor et al. (2004)
CRIT_LAI_T	LAI below which transpiration is physiologically limited	0.7	Challinor et al. (2004)
P_TRANS_MAX	Max value of potential transpiration	0.3 cm/day	Challinor et al. (2004)
VPD_CTE	Used to calculate vapour pressure deficit	0.7	Challinor et al. (2004)

VPD_REF	Used to calculate Priestly-Taylor coefficient	1 kPa	Challinor et al. (2004)
SHF_CTE	Used to calculate soil heat flux	0.4	Choudhury et al. (1987)
EXTC	Extinction coefficient	0.5	Challinor et al. (2004)
Soil and roots			
ASWS	Initial soil water (fraction of water holding capacity)	0.7	Watson et al. (2015)
NWBDAYS	Number of days water balance is run before start of planting window	30 days	N/a
NSL	Number of soil layers	25	Challinor et al. (2004)
ZSMAX	Maximum rooting depth	210 cm	Challinor et al. (2004)
RKCTE	Used to calculate saturated hydraulic conductivity of the soil	75 cm/day	Suleiman and Ritchie (2001)
UPDIFC	Uptake diffusion coefficient	0.06 cm2/day	Challinor et al. (2004)
EFV	Extraction front velocity	1 cm/day	Challinor et al. (2004)
DLDLAI	Increase in root length density at surface with LAI	1 cm/cm3	Challinor et al. (2004)
RLVEF	Root length density at the extraction front	0.3 cm/cm	Challinor et al. (2004)
Biomass and yield			
TE	Transpiration efficiency	1.7 Pa	Challinor et al. (2004)
TENMAX	Max. normalised transpiration efficiency	3 g/kg	Challinor et al. (2004)
RUE	Radiation Use Efficiency	1.7 (g/MJ)	Ramirez-Villegas et al. (2017)
DHDT	Maximum daily increase in harvest index	0.007	Challinor et al. (2004)
MAX_HI_GNUT	Maximum harvest index for groundnut	0.67	Nigam et al. (2001)

Development			
FSWSOW	Fractional soil moisture for intelligent planting and emergence	0.5	Challinor et al. (2004)
IEMDAY	Number of days from planting to emergence	8	Challinor et al. (2004)
I_TTCALC	Shape of function to calculate thermal time	0 (triangular)	Challinor et al. (2004)
TBGNUT	Base temperature for maize	10C	Challinor et al. (2004)
TOGNUT	Optimum temperature for maize	28C	Challinor et al. (2004)
TMGNUT	Maximum temperature for maize	50C	Challinor et al. (2004)
GCPLFL	Thermal time from planting to flowering	340-425 degree days	Challinor et al. (2004); Nicklin (2013)
GCFLPF	Flowering to beginning of grain-filling	255-330 degree days	Challinor et al. (2004); Nicklin (2013)
GCPFLM	Beginning of grain-filling to maximum LAI	200-502 degree days	Challinor et al. (2004); Nicklin (2013)
GCLMHA	Maximum LAI to physiological maturity	500-750 degree days	Challinor et al. (2004); Nicklin (2013)
Optional processes			
TETRS	Switch for temperature dependence of TE and RUE	1 (on)	N/a
TETR1	Temperature above which TE and RUE begin linear reduction	35 C	Challinor et al. (2009)
TETR2	Temperature above which TE and RUE are zero	47 C	Challinor et al. (2009)
HTS	Switch for heat stress around flowering	2	N/a

TSETCRIT	Switch for high temperature stress around flowering	34	Challinor et al. (2007)
TSETZERO	Switch for high temperature stress around flowering	44	Challinor et al. (2007)
TDS	Switch for terminal drought stress (TDS)	1 (on)	N/a
HIMIN	Minimum harvest index for TDS to occur	0.25	Challinor et al. (2009)
SWCFAC	Fraction of water holding capacity below which TDS occurs	0.05	Challinor et al. (2009)
I_EMER	Switch for intelligent emergence	1 (on)	N/a
TRKILL	Switch for lethal temperature parameterisation	1 (on)	N/a
TRKILL1	Temperature below which crop fails	0;	N/a
TRKILL2	Temperature above which crop fails	47	Challinor et al. (2009)
WS	Switch for water stress around flowering	2 (on)	Challinor et al. (2006)
SWFFTHR	SWFAC threshold for damage to flowers	0.2	Challinor et al. (2006)
TRLAI	Switch for temperature dependence of LAI growth	-1 (off)	N/a

Table S4: Parameters used in GLAM-soybean, with ranges where applicable.

Parameter	Explanation	Value (range)	Reference
Leaves			
DLDTMX	Maximum daily increase in LAI	0.16	Osborne et al. (2013)

SWF_THRESH	Critical value of soil water stress factor for leaves	0.7	Osborne et al. (2013)
NDSLA	Specific Leaf Area control	5 days	Challinor and Wheeler (2008)
SLA_INI	Specific leaf area control (see Challinor and Wheeler 2008)	300 cm2/g	Osborne et al. (2013)
MAX_ISTG_SLA	Max development stage for SLA control	2 (until flowering)	N/a
Evaporation and transpiration			
ALBEDO	Albedo	0.2	Challinor et al. (2004)
CRIT_LAI_T	LAI below which transpiration is physiologically limited	4.6	Osborne et al. (2013)
P_TRANS_MAX	Max value of potential transpiration	0.38 cm/day (0.2-0.73)	Osborne et al. (2013)
VPD_CTE	Used to calculate vapour pressure deficit	0.7 (0.42 to 0.98)	Tanner and Sinclair (1983)
VPD_REF	Used to calculate Priestly-Taylor coefficient	1 kPa (0.6-1.4)	Steiner et al. (1991)
SHF_CTE	Used to calculate soil heat flux	0.4	Choudhury et al. (1987)
EXTC	Extinction coefficient	0.5	Osborne et al. (2013)
Soil and roots			
ASWS	Initial soil water (fraction of water holding capacity)	0.7	Watson et al. (2015)
NWBDAYS	Number of days water balance is run before start of planting window	30 days	N/a
NSL	Number of soil layers	25	Challinor et al. (2004)
ZSMAX	Maximum rooting depth	100 cm	Osborne et al. (2013)
RKCTE	Used to calculate saturated hydraulic conductivity of the soil	75 cm/day	Suleiman and Ritchie (2001)

UPDIFC	Uptake diffusion coefficient	0.25 cm2/day (0.19 to 0.3)	Jamieson and Ewert (1999); Robertson and Fukai (1994)
EFV	Extraction front velocity	1 cm/day	Osborne et al. (2013)
DLDLAI	Increase in root length density at surface with LAI	1 cm/cm3	Osborne et al. (2013)
RLVEF	Root length density at the extraction front	0.5 cm/cm	Osborne et al. (2013)
Biomass and yield			
TE	Transpiration efficiency	1.8 Pa	Osborne et al. (2013)
TENMAX	Max. normalised transpiration efficiency	3 g/kg	Osborne et al. (2013)
RUE	Radiation Use Efficiency	1.4 (g/MJ)	Osborne et al. (2013)
DHDT	Maximum daily increase in harvest index	0.0077	Osborne et al. (2013)
MAX_HI_SOYBEAN	Maximum harvest index for soybean	0.6	Spaeth and Sinclair (1985)
Development			
FSWSOW	Fractional soil moisture for intelligent planting and emergence	0.5	Challinor et al. (2004)
IEMDAY	Number of days from planting to emergence	10	Osborne et al. (2013)
I_TTCALC	Shape of function to calculate thermal time	0 (triangular)	Osborne et al. (2013)
TBSOY	Base temperature for soybean	6.5C	Osborne et al. (2013); Hatfield et al. (2011); Setiyono et al. (2007)
TOSOY	Optimum temperature for soybean	26C for stage 1; 21.5 for other stages	Osborne et al. (2013); Hatfield et al. (2011); Setiyono et al. (2007)
TMSOY	Maximum temperature for soybean	35C for stage 1; 38.5 for other stages	Osborne et al. (2013); Hatfield et al. (2011); Setiyono et al. (2007)
GCSOPLFL	Thermal time for stage 1 (planting to flowering)	346-477 degree days	Osborne et al. (2013)

GCSOFLPO	Thermal time for stage 2 (flowering to beginning of pod-filling)	285-380 degree days	Osborne et al. (2013)
GCSOPOML	Thermal time for stage 3 (Beginning of pod-filling to maximum LAI)	19-342 degree days	Osborne et al. (2013)
GCSOMLMA	Thermal time for stage 4 (Maximum LAI to physiological maturity)	413-865 degree days	Osborne et al. (2013)
CRITPP	Critical photoperiod	11.91-14.48	Osborne et al. (2013)
PPSEN	Photoperiod sensitivity	0.188-0.34	Osborne et al. (2013)
Optional processes			
TETRS	Switch for temperature dependence of TE and RUE	1 (on)	N/a
TETR1	Temperature above which TE and RUE begin linear reduction	31 C	Osborne et al. (2013)
TETR2	Temperature above which TE and RUE are zero	39 C	Luo (2011)
TETR3	Temperature below which TE and RUE are zero	0 C	Van Heerden et al. (2003)
TETR4	Temperature below which TE and RUE begin linear reduction	15 C	Van Heerden et al. (2003)
HTS	Switch for heat stress around flowering	2	Osborne et al. (2013)
TSETCRIT	Switch for high temperature stress around flowering	31	Osborne et al. (2013)
TSETZERO	Switch for high temperature stress around flowering	36	Osborne et al. (2013)
TDS	Switch for terminal drought stress (TDS)	1 (on)	N/a

HIMIN	Minimum harvest index for TDS to occur	0.25	Challinor et al. (2009)
SWCFAC	Fraction of water holding capacity below which TDS occurs	0.05	Challinor et al. (2009)
I_EMER	Switch for intelligent emergence	1 (on)	N/a
TRKILL	Switch for lethal temperature parameterisation	-1 (off)	N/a
WS	Switch for water stress around flowering	2 (on)	N/a
SWFFTHR	SWFAC threshold for damage to flowers	0.2	Challinor et al. (2006)
TRLAI	Switch for temperature dependence of LAI growth	-1 (off)	N/a

Table S5. Scenario assumptions, as informed by stakeholders. HT = High tech. / high land reform / high market function / high policy effectivess scenarios, LT = the corresponding Low scenarios. Agricultural land changes - if no percentage increase is specified, all available (i.e. not forested, urban or protected land) is used for agriculture in 2050. Crop diversity - if a percentage increase is given, this is the proportion of maize land going to other crops; if a percentage decrease is given, this is the proportion of extra maize land prescribed; if no percentage change is specified, full diversification or the reciprocal is modelled, as described in Section 1.3. Irrigation - if an increase is specified, all future areas are irrigated.

South Africa	RCP8.5, HT	RCP8.5, LT	RCP2.6, HT	RCP2.6, LT
1). Arable crop area	10% decrease	10% increase	10% decrease	No change
2). Livestock pasture	15% decrease	10% decrease	10% increase	10% increase
3). Crop diversity	25% increase	25% increase	10% increase	10% increase
4). Irrigation	All areas irrigated	All areas irrigated	No change	No change
5). Trade	Decrease exports. Increase imports	Decrease exports. Increase imports	Increase Exports. Increase imports	Increase exports. Imports no change.
Zambia	RCP8.5, HT	RCP8.5, LT	RCP2.6, HT	RCP2.6, LT
1). Arable crop area	5% increase	10% decrease	5% increase	no change
2). Livestock pasture	Increase (by about 5%)	no change	Increase (by about 25%)	no change
3). Crop diversity	Decrease	Increase	Increase	Increase
4). Irrigation	Increase	Increase	Increase	No change
5). Trade	Increase imports	Increase import	Increase exports	No hange
Tanzania	RCP8.5, HT	RCP8.5, LT	RCP2.6, HT	RCP2.6, LT
1). Arable crop area	Increase	Increase	increase	Increase
2). Livestock pasture	Increase (half of arable increase)	Increase	Increase	Increase
3). Crop diversity	Decrease (50%)	Decrease (50%)	Increase (50%)	Increase (50%)
4). Irrigation	Increase	Decrease (All rainfed in 2050)	Increase	No change
5). Trade	Increase imports and exports.	Increase imports. Decrease exports.	Increase exports. Decrease imports.	Increase imports. Decrease exports.
Malawi	RCP8.5, HT	RCP8.5, LT	RCP2.6, HT	RCP2.6, LT
1). Arable crop area	Increase	10% decrease	Increase	No change
2). Livestock Pasture	Increase	10% decrease	Increase	No change
3). Crop diversity	Increase	No change	Increase	No change
4). Irrigation	Increase	No change	Increase	No change
5). Trade	Increase imports. Increase exports.	Increase imports. Decrease exports.	Increase exports	No change

Table S6. FAO Food Balance Sheets (FBS) quantify the mass of food supply per food item, broken down as follows. *calculated using data from Gustavsson J, Cederberg C, Sonesson U, van Otterdijk R and Meybeck A. (2011) Global food losses and food waste: extent, causes and prevention. FAO, Rome (data not in the FBS)

	Production
plus	Imports
less	Exports
plus	Stock variation
equals	**Domestic Supply Quantity**
less	Processing
less	Feed
less	Seed
less	Losses
less	Other uses
equals	**Food for human consumption**
less	Avoidable household waste*
equals	**Food after avoidable household waste***

1.8.1 Figures

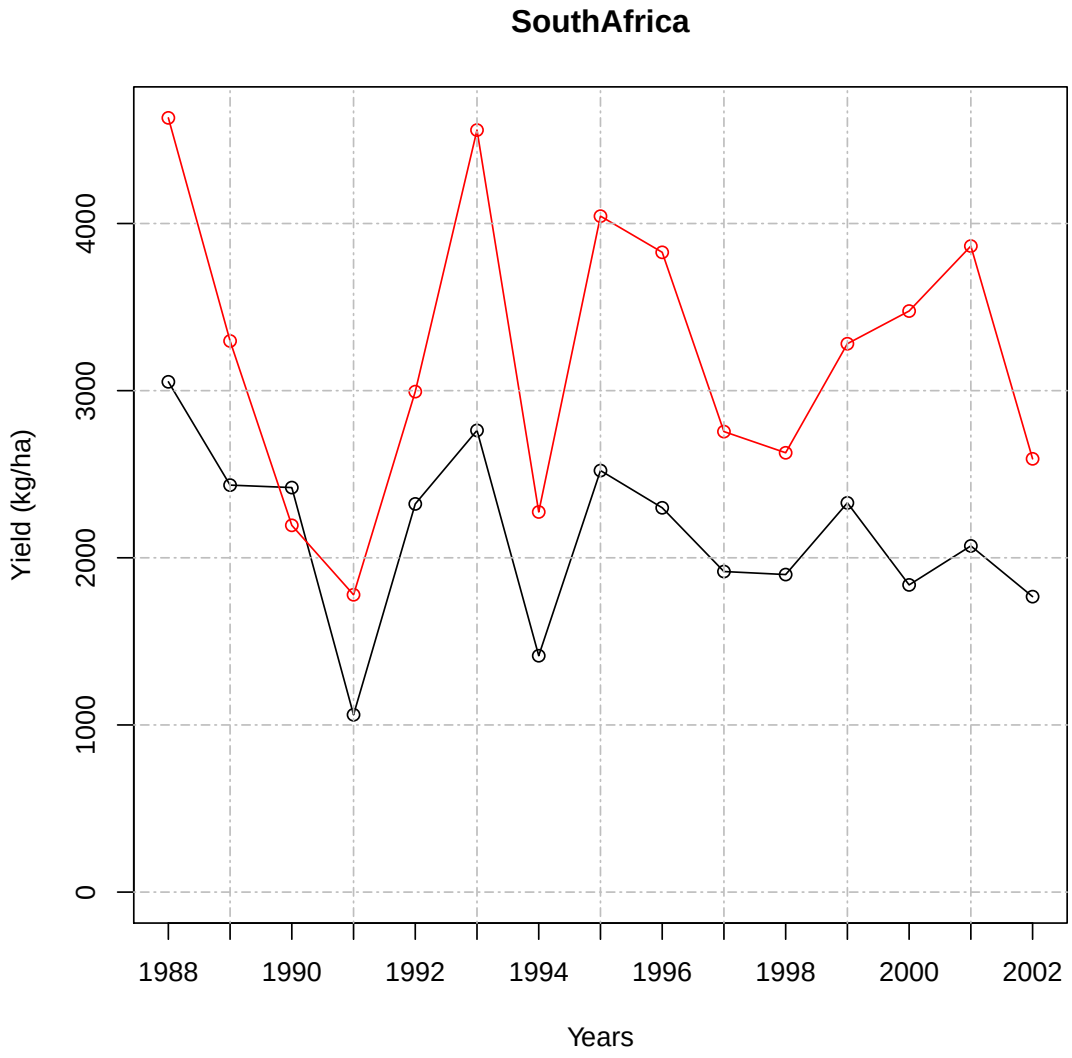

Figure S1. Observed and simulated yields using the weighted yield mean approach.

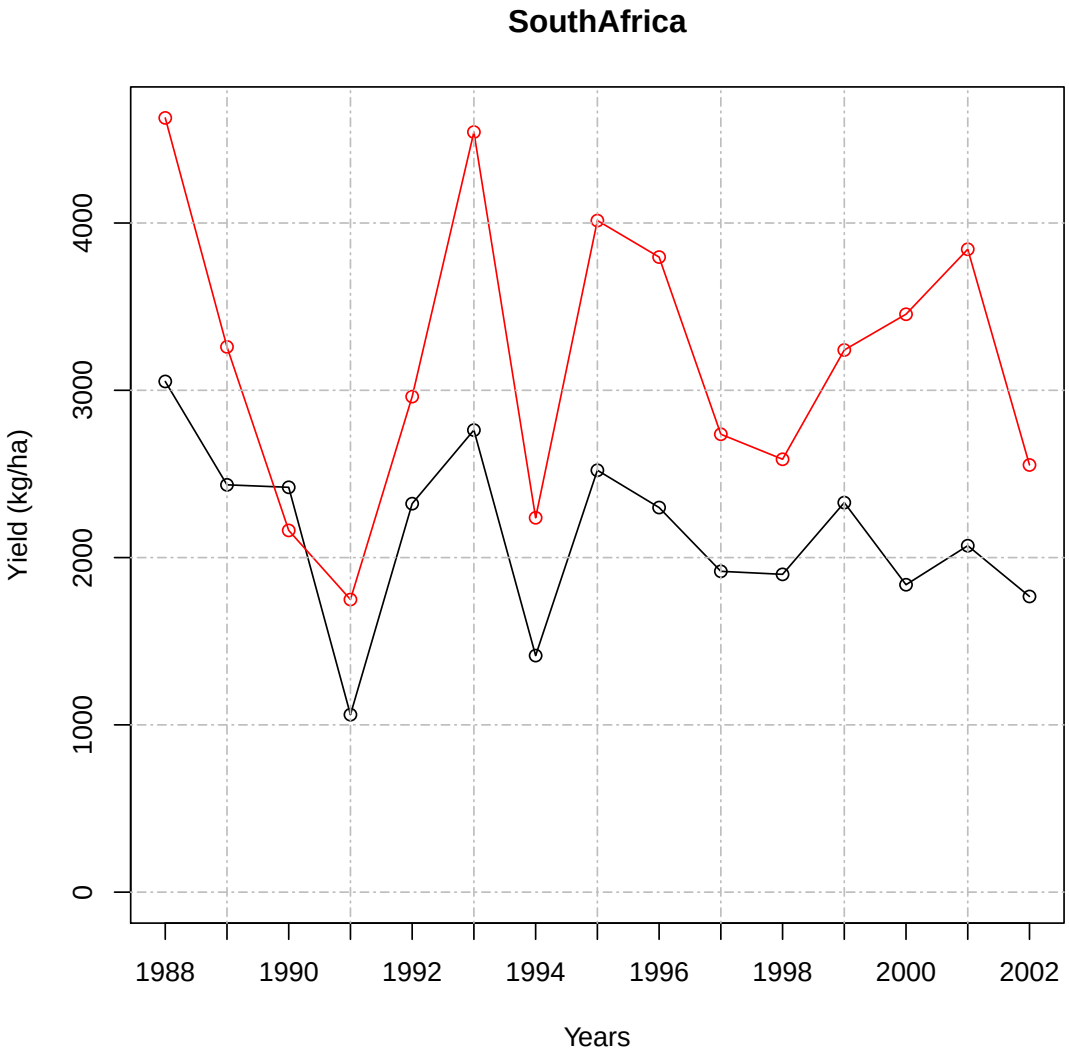

Figure S2. Observed and simulated yields using the supplementary irrigation and majority grid cell approach.

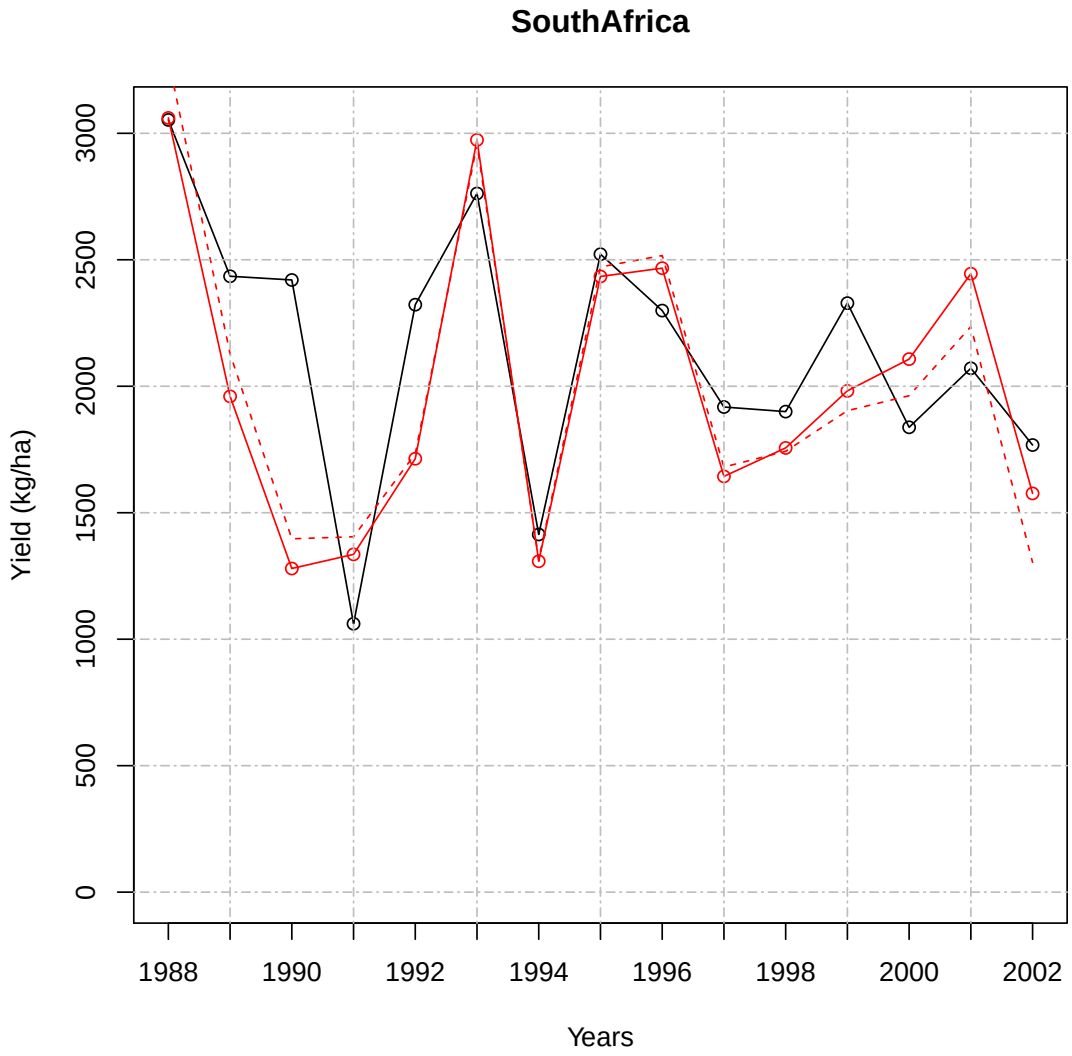

Figure S3. South Africa observed yields (black line) and simulated detrended yields (red line - dashed red line is non-detrended simulated yields). Correlation coefficient between detrended observed and simulated yields is 0.73, p-value 0.002.

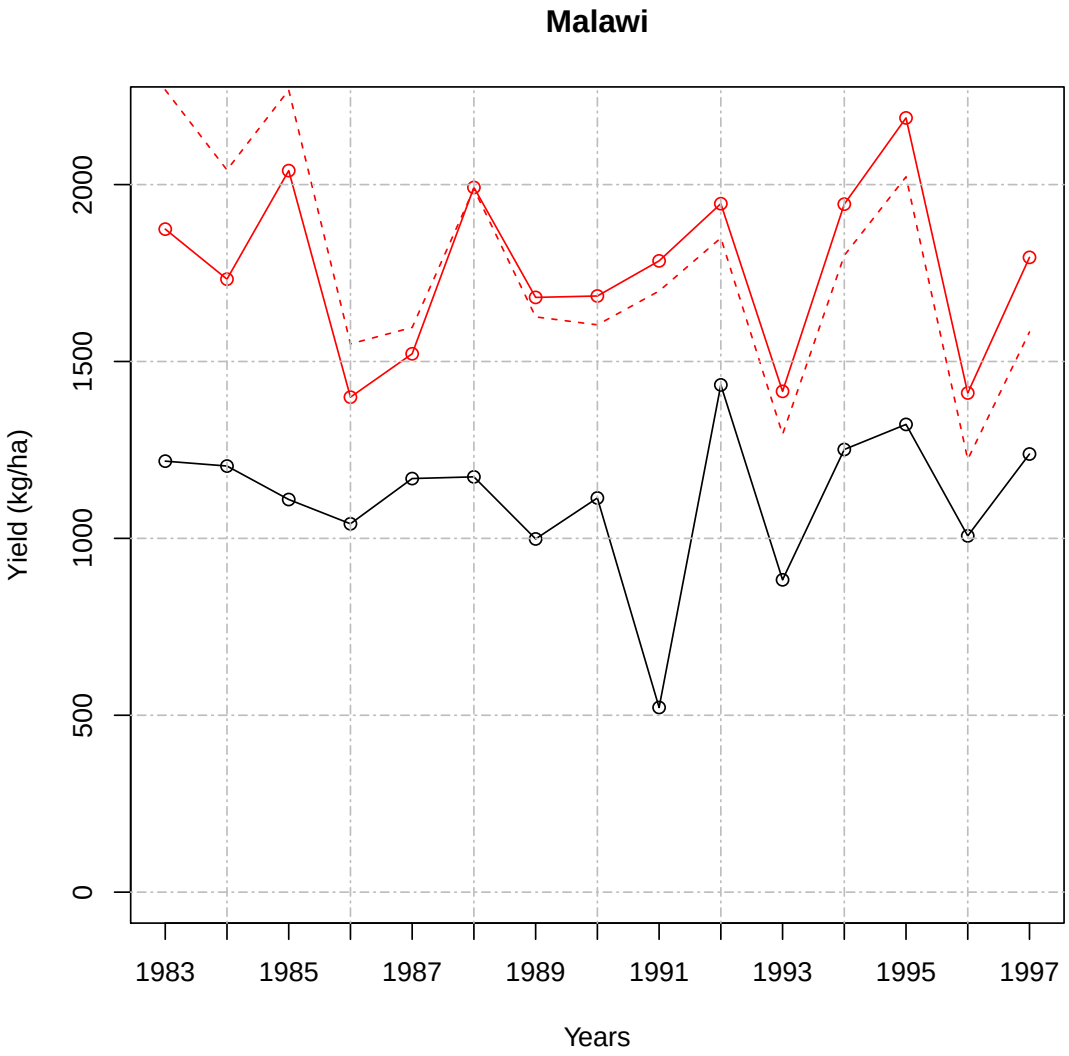

Figure S4. Malawi observed yields (black line) and simulated detrended yields (red line - dashed red line is non-detrended simulated yields). Correlation coefficient between detrended observed and simulated yields is 0.444, p-value 0.097.

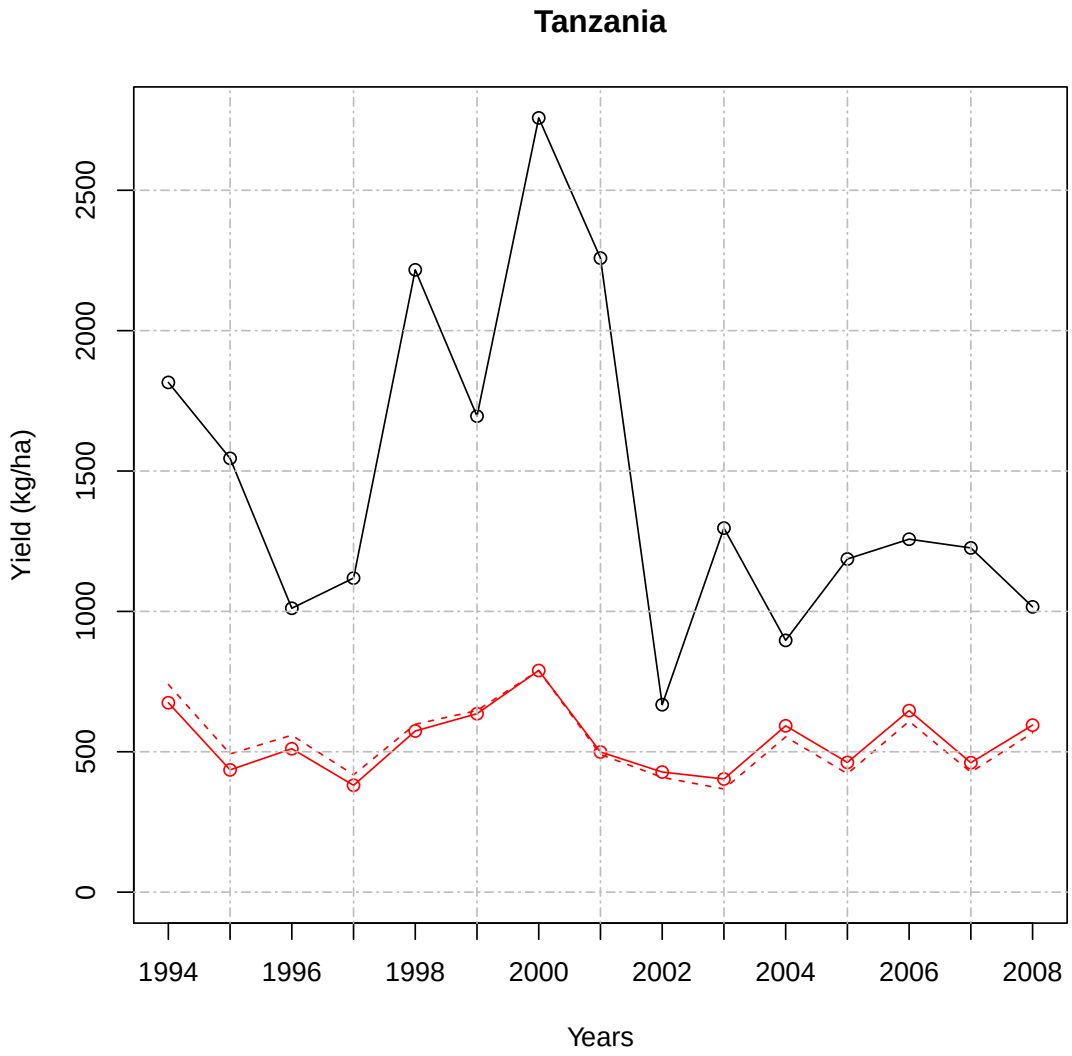

Figure S5. Tanzania observed yields (black line) and simulated detrended yields (red line - dashed red line is non-detrended simulated yields). Correlation coefficient between detrended observed and simulated yields is 0.55, p-value 0.03.

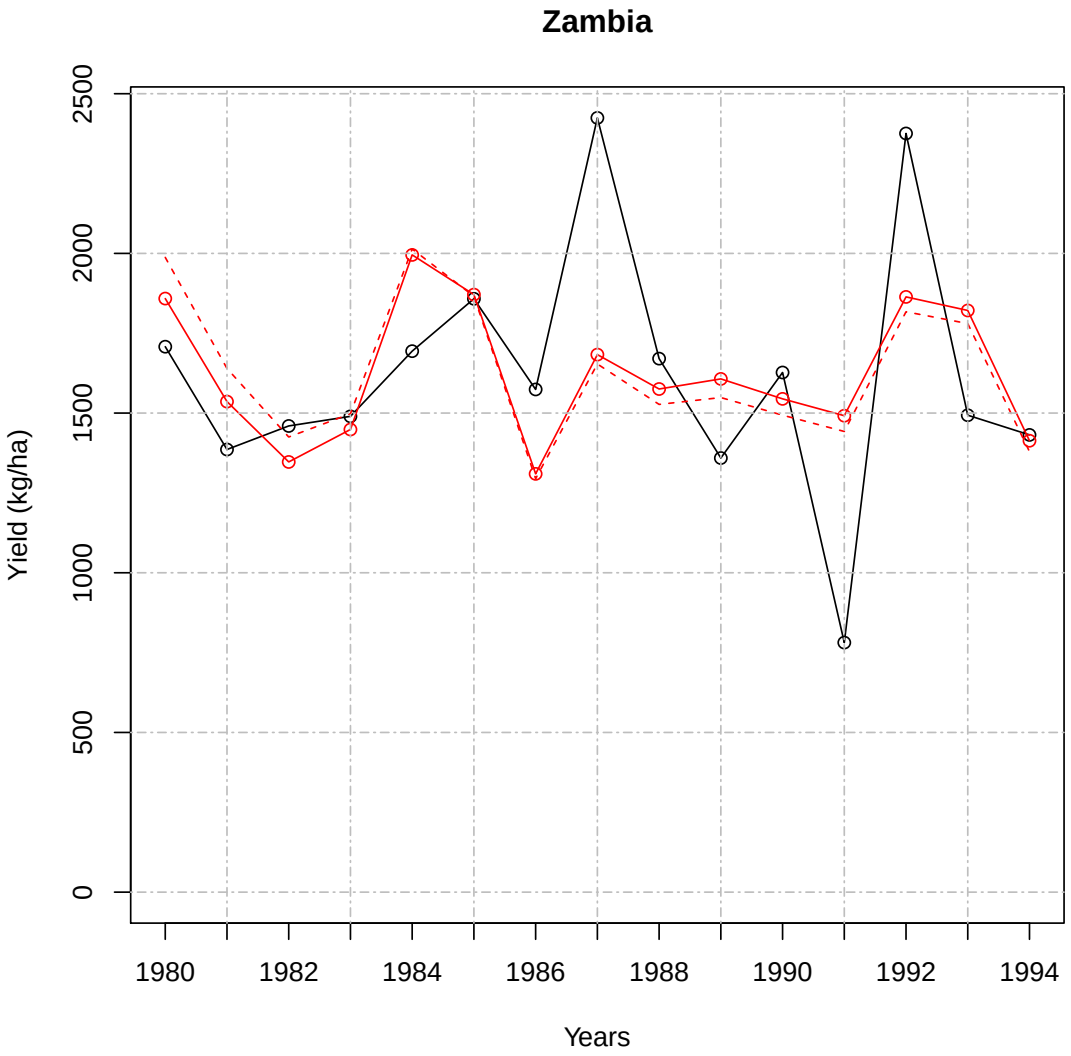

Figure S6. Zambia observed yields (black line) and simulated detrended yields (red line - dashed red line is non-detrended simulated yields). Correlation coefficient between detrended observed and simulated yields is 0.475, p-value 0.073.

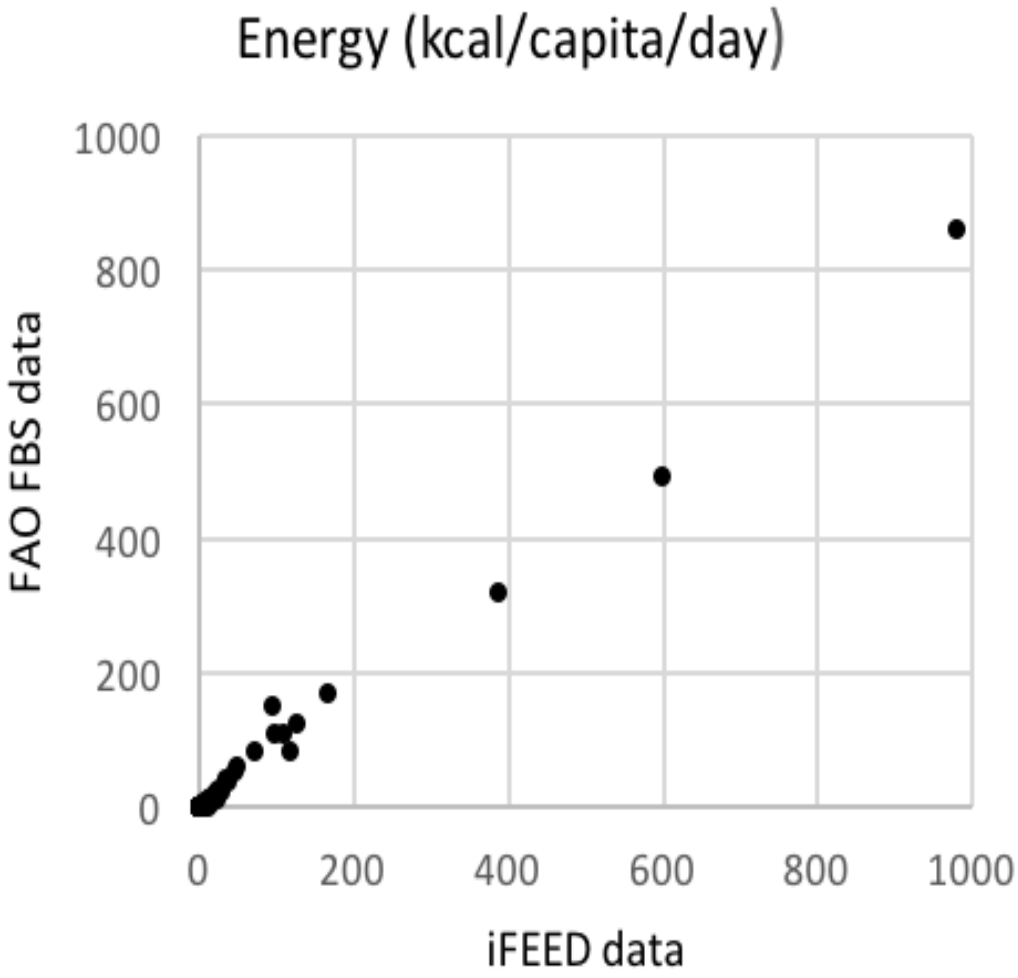

Figure S7. Comparison of FAO Food Balance Sheet and iFEED-calculated values for energy in South Africa.

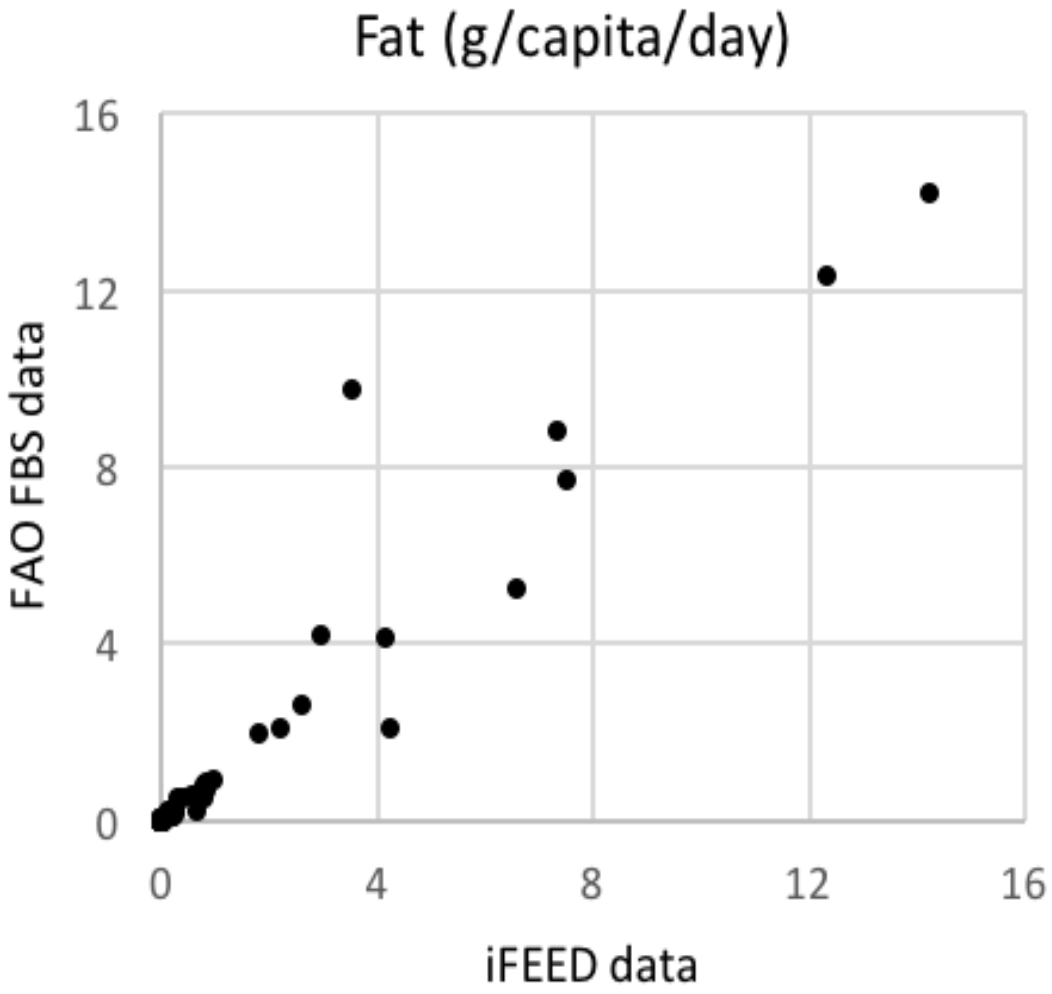

Figure S8. Comparison of FAO Food Balance Sheet and iFEED-calculated values for fat in South Africa.

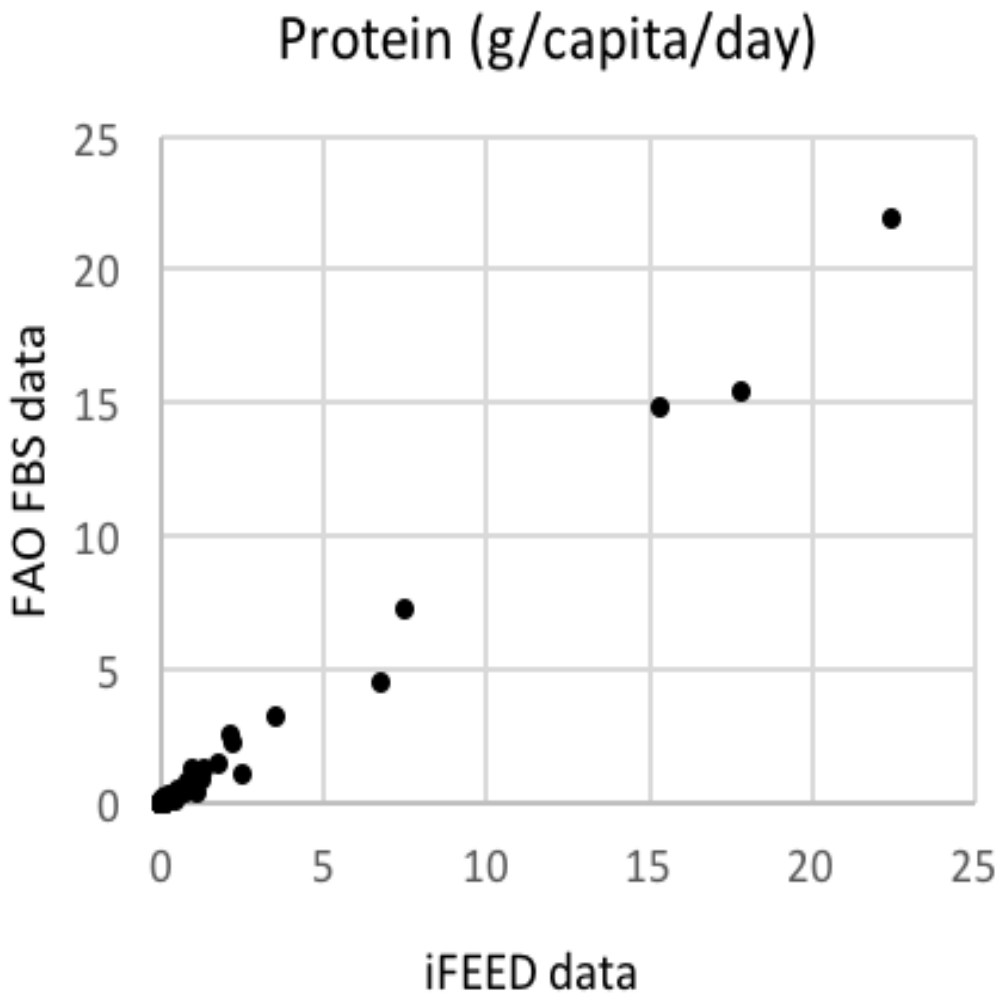

Figure S9. Comparison of FAO Food Balance Sheet and iFEED-calculated values for protein in South Africa.

REFERENCES

Adamtey, N., Cofie, O., Ofosu-Budu, K., Ofosu-Anim, J., Laryea, K., and Forster, D. (2010). Effect of n-enriched co-compost on transpiration efficiency and water-use efficiency of maize (zea mays l.) under controlled irrigation. *Agricultural Water Management* 97, 995–1005

Al-Kaisi, M., Brun, L. J., and Enz, J. W. (1989). Transpiration and evapotranspiration from maize as related to leaf area index. *Agricultural and Forest Meteorology* 48, 111–116

Allen, E. and Scott, R. K. (1980). An analysis of growth of the potato crop. *The Journal of Agricultural Science* 94, 583–606

Anderson, W., You, L., Wood, S., Wood-Sichra, U., and Wu, W. (2015). An analysis of methodological and spatial differences in global cropping systems models and maps. *Global Ecology and Biogeography* 24, 180–191

Asfaw, D., Black, E., Brown, M., Nicklin, K. J., Otu-Larbi, F., Pinnington, E., et al. (2018). TAMSAT-ALERT v1: A new framework for agricultural decision support. *Geoscientific Model Development* 11, 2353–2371

Ashagre, H., Hamza, I., Tesfaye, B., Derebachew, D., Ayana, B., and Tilahun, D. (2001). Emergence and Seedling Growth of Corn (Zea mays L.) as Influenced by Irrigation Schedules on Vertisol. *College of Agriculture and Veterinary Sciences, Department of Plant Sciences and Horticulture, Ambo University*

Ashraf, M. and Hafeez, M. (2004). Thermotolerance of pearl millet and maize at early growth stages: growth and nutrient relations. *Biologia Plantarum* 48, 81–86

Bergamaschi, H., Costa, S. M. S. D., Wheeler, T. R., and Challinor, A. J. (2013). Simulating maize yield in sub-tropical conditions of southern Brazil using GLAM model. *Pesquisa Agropecuária Brasileira* 48, 132–140

[Dataset] Calton, S. J. M.-D. L. T. A., B. (2016). Water Resource Reanalysis v1: Data Access and Model Verification Results. doi:https://doi.org/10.5281/zenodo.57760

Campbell, M. D., Campbell, G. S., Kunkel, R., and Papendick, R. I. (1976). A model describing soil-plant-water relations for potatoes. *American Potato Journal* , 431–441

Carberry, P., Muchow, R., and McCown, R. (1989). Testing the CERES-Maize simulation model in a semi-arid tropical environment. *Field Crops Research* 20, 297–315

Challinor, A., Muller, C., Asseng, S., Deva, C., Nicklin, K., Wallach, D., et al. (2018). Improving the use of crop models for risk assessment and climate change adaptation. *Agricultural Systems* 159, 296–306

Challinor, A., Slingo, J., Wheeler, T., Craufurd, P., and Grimes, D. (2003). Toward a combined seasonal weather and crop productivity forecasting system: determination of the working spatial scale. *Journal of Applied Meteorology* 42, 175–192

Challinor, A. and Wheeler, T. (2008). Use of a crop model ensemble to quantify CO2 stimulation of water-stressed and well-watered crops. *Agricultural and Forest Meteorology* 148, 1062 – 1077. doi:http://dx.doi.org/10.1016/j.agrformet.2008.02.006

Challinor, A., Wheeler, T., Craufurd, P., Ferro, C., and Stephenson, D. (2007). Adaptation of crops to climate change through genotypic responses to mean and extreme temperatures. *Agriculture, Ecosystems & Environment* 119, 190–204

Challinor, A., Wheeler, T., Craufurd, P., Slingo, J., and Grimes, D. (2004). Design and optimisation of a large-area process-based model for annual crops. *Agricultural and Forest Meteorology* 124, 99–120. doi:10.1016/j.agrformet.2004.01.002

Challinor, A., Wheeler, T., Osborne, T., and Slingo, J. (2006). Assessing the vulnerability of crop productivity to climate change thresholds using an integrated crop-climate model

Challinor, A., Wheeler, T., Slingo, J., and Hemming, D. (2005). Quantification of physical and biological uncertainty in the simulation of the yield of a tropical crop using present-day and doubled CO2 climates. *Philosophical Transactions of the Royal Society of London B: Biological Sciences* 360, 2085–2094

Challinor, A. J., Koehler, A.-K., Ramirez-Villegas, J., Whitfield, S., and Das, B. (2016). Current warming will reduce yields unless maize breeding and seed systems adapt immediately. *Nature Climate Change* 6, 954–958

Challinor, A. J., Wheeler, T., Hemming, D., and Upadhyaya, H. D. (2009). Ensemble yield simulations: crop and climate uncertainties, sensitivity to temperature and genotypic adaptation to climate change. *Climate Research* 38, 117–127. doi:10.3354/cr00779

Choudhury, B., Idso, S., and Reginato, R. (1987). Analysis of an empirical model for soil heat flux under a growing wheat crop for estimating evaporation by an infrared-temperature based energy balance equation. *Agricultural and Forest Meteorology* 39, 283–297

Dardanelli, J. L., Bachmeier, O. A., Sereno, R., and Gil, R. (1997). Rooting depth and soil water extraction patterns of different crops in a silty loam haplustoll. *Field Crops Research* 54, 29–38

Dee, D. P., Uppala, S., Simmons, A., Berrisford, P., Poli, P., Kobayashi, S., et al. (2011). The ERA-Interim reanalysis: Configuration and performance of the data assimilation system. *Quarterly Journal of the Royal Meteorological Society* 137, 553–597

Droutsas, I., Challinor, A. J., Swiderski, M., and Semenov, M. A. (2019). New modelling technique for improving crop model performance - Application to the GLAM model. *Environmental Modelling & Software* 118, 187–200

Durand, J.-L., Delusca, K., Boote, K., Lizaso, J., Manderscheid, R., Weigel, H. J., et al. (2017). How accurately do maize crop models simulate the interactions of atmospheric CO2 concentration levels with limited water supply on water use and yield? *European Journal of Agronomy*

Ejieji, C. and Gowing, J. (2000). A dynamic model for responsive scheduling of potato irrigation based on simulated water-use and yield. *The Journal of Agricultural Science* 135, 161–171

Ewing, E. E. and Wareing, P. F. (1978). Shoot, stolon, and tuber formation on potato (solanum tuberosum l.) cuttings in response to photoperiod. *Plant Physiology* 61, 348–353

Famien, A. M., Janicot, S., Ochou, A. D., Vrac, M., Defrance, D., Sultan, B., et al. (2018). A bias-corrected CMIP5 dataset for Africa using the CDF-t method: a contribution to agricultural impact studies. *Earth System Dynamics* 9, 313–338

FAO (2019). FAOSTAT, FAO Statistical Databases

Fasan, T. and Haverkort, A. (1991). The influence of cyst nematodes and drought on potato growth. 1. Effects on plant growth under semi-controlled conditions. *Netherlands Journal of Plant Pathology* 97, 151–161

Frieler, K., Lange, S., Piontek, F., Reyer, C. P., Schewe, J., Warszawski, L., et al. (2017). Assessing the impacts of 1.5 C global warming–simulation protocol of the Inter-Sectoral Impact Model Intercomparison Project (ISIMIP2b). *Geoscientific Model Development*

Ghalanos, A. and Theussl, S. (2015). *Rsolnp: General Non-linear Optimization Using Augmented Lagrange Multiplier Method*. R package version 1.16.

Gourdji, S. M., Sibley, A. M., and Lobell, D. B. (2013). Global crop exposure to critical high temperatures in the reproductive period: historical trends and future projections. *Environmental Research Letters* 8, 024041

Hatfield, J. L., Boote, K. J., Kimball, B., Ziska, L., Izaurralde, R. C., Ort, D., et al. (2011). Climate impacts on agriculture: implications for crop production. *Agronomy Journal* 103, 351–370

Haverkort, A. J., Uenk, D., Veroude, H., and Van De Waart, M. (1991). Relationships between ground cover, intercepted solar radiation, leaf area index and infrared reflectance of potato crops. *Potato Research* 34, 113–121. doi:10.1007/BF02358105

Hay, R. and Gilbert, R. (2001). Variation in the harvest index of tropical maize: evaluation of recent evidence from Mexico and Malawi. *Annals of Applied Biology* 138, 103–109

Hay, R. and Porter, J. (2006). *The physiology of crop yield* (Blackwell Publishing)

Herrero, M., Havlík, P., Valin, H., Notenbaert, A., Rufino, M. C., Thornton, P. K., et al. (2013). Biomass use, production, feed efficiencies, and greenhouse gas emissions from global livestock systems. *Proceedings of the National Academy of Sciences* 110, 20888–20893

Ingram, K. T. and McCloud, D. E. (1984). Simulation of Potato Crop Growth and Development. *Crop Science* 24, 21. doi:10.2135/cropsci1984.0011183X002400010006x

Iwama, K., Hukushima, T., Yoshimura, T., and Nakaseko, K. (1993). Influence of planting density on root growth and yield in potato. *Japanese Journal of Crop Science* 62, 628–635

Jamieson, P. and Ewert, F. (1999). The role of roots in controlling soil water extraction during drought: an analysis by simulation. *Field Crops Research* 60, 267–280

Jefferies, R. (1993). Use of a simulation model to assess possible strategies of drought tolerance in potato (*Solanum tuberosum* L.). *Agricultural Systems* 41, 93–104

Jefferies, R. and MacKerron, D. (1989). Radiation interception and growth of irrigated and droughted potato (*Solanum tuberosum*). *Field Crops Research* 22, 101–112

Jefferies, R. A. and Heilbronn, T. D. (1991). Water stress as a constraint on growth in the potato crop. 1. Model development. *Agricultural and Forest Meteorology* 53, 185–196. doi:http://dx.doi.org/10.1016/0168-1923(91)90056-V

Jefferies, R. A. and Mackerron, D. K. L. (1987). Thermal time as a non-destructive method of estimating tuber initiation in potatoes , 249–252

Jennings, S. A., Koehler, A.-K., Nicklin, K. J., Deva, C., Sait, S. M., and Challinor, A. J. (2020). Global potato yields increase under climate change with adaptation and CO2 fertilisation. *Frontiers in Sustainable Food Systems* 4

Jones, J. L. and Allen, E. J. (1983). Effects of date of planting on plant emergence, leaf growth, and yield in contrasting potato varieties. *The Journal of Agricultural Science* 101, 81–95. doi:10.1017/S002185960003639X

Jongschaap, R. E. E. and Booij, R. (2004). Spectral measurements at different spatial scales in potato: relating leaf, plant and canopy nitrogen status. *International Journal of Applied Earth Observation and Geoinformation* 5, 205–218. doi:http://dx.doi.org/10.1016/j.jag.2004.03.002

Kaminski, K. P., Kørup, K., Kristensen, K., Nielsen, K., Liu, F., Topbjerg, H. B., et al. (2015). Contrasting Water-Use Efficiency (WUE) Responses of a Potato Mapping Population and Capability of Modified Ball-Berry Model to Predict Stomatal Conductance and WUE Measured at Different Environmental Conditions. *Journal of Agronomy and Crop Science* 201, 81–94

Keating, B., Wafula, B., and Watiki, J. (1992). Development of a modelling capability for maize in semi-arid eastern Kenya. In *A Search for Strategies for Sustainable Dryland Cropping in Semi-arid Eastern Kenya. ACIAR Proceedings*. vol. 41, 26–33

Khurana, S. and McLaren, J. (1982). The influence of leaf area, light interception and season on potato growth and yield. *Potato Research* 25, 329–342

Kimball, B. A. (2016). Crop responses to elevated CO2 and interactions with H2O, N, and temperature. *Current Opinion in Plant Biology* 31, 36–43

Kiniry, J., Jones, C., O'toole, J., Blanchet, R., Cabelguenne, M., and Spanel, D. (1989). Radiation-use efficiency in biomass accumulation prior to grain-filling for five grain-crop species. *Field Crops Research* 20, 51–64

Lange, S. (2018). Bias correction of surface downwelling longwave and shortwave radiation for the EWEMBI dataset. *Earth System Dynamics* 9, 627–645

[Dataset] Lange, S. (2019). EartH2Observe, WFDEI and ERA-Interim data Merged and Bias-corrected for ISIMIP (EWEMBI). doi:http://doi.org/10.5880/pik.2019.004

Lesczynski, D. and Tanner, C. (1976). Seasonal variation of root distribution of irrigated, field-grown Russet Burbank potato. *American Potato Journal* 53, 69–78

Lindquist, J. L., Arkebauer, T. J., Walters, D. T., Cassman, K. G., and Dobermann, A. (2005). Maize radiation use efficiency under optimal growth conditions. *Agronomy Journal* 97, 72–78

Lobell, D. B. (2014). Climate change adaptation in crop production: Beware of illusions. *Global Food Security* 3, 72–76

Long, S. P., Ainsworth, E. A., Leakey, A. D., Nösberger, J., and Ort, D. R. (2006). Food for thought: lower-than-expected crop yield stimulation with rising co2 concentrations. *science* 312, 1918–1921

Luo, Q. (2011). Temperature thresholds and crop production: a review. *Climatic Change* 109, 583–598

Manrique, L. A. and Hodges, T. (1989). Estimation of tuber initiation in potatoes grown in tropical environments based on different methods of computing thermal time. *American Potato Journal* 66, 425–436

Monteith, J. and Unsworth, M. (2007). *Principles of Environmental Physics* (Academic Press)

Moriondo, M., Bindi, M., and Sinclair, T. (2005). Analysis of Solanaceae Species Harvest-organ Growth by Linear Increase in Harvest Index and Harvest-organ Growth Rate. *Journal of the American Society for Horticultural Science* 130, 799–805

Müller, C. and Robertson, R. D. (2014). Projecting future crop productivity for global economic modeling. *Agricultural Economics* 45, 37–50

Naiken, L. (2014). Methodological issues in the estimation of the prevalence of undernourishment based on dietary energy consumption data: a review and clarification. *Statistics Division Working Paper no. ESS/14-03, FAO, Rome*

Nicklin, K. J. (2013). Seasonal crop yield forecasting in semi-arid West Africa. *PhD Thesis, University of Leeds*

Nigam, S., Upadhyaya, H., Chandra, S., Rao, R. N., Wright, G., and Reddy, A. (2001). Gene effects for specific leaf area and harvest index in three crosses of groundnut (Arachis hypogaea). *Annals of Applied Biology* 139, 301–306

Osborne, T., Rose, G., and Wheeler, T. (2013). Variation in the global-scale impacts of climate change on crop productivity due to climate model uncertainty and adaptation. *Agricultural and Forest Meteorology* 170, 183–194. doi:10.1016/j.agrformet.2012.07.006

Parker, C., Carr, M., Jarvis, N., Evans, M., and Lee, V. (1989). Effects of subsoil loosening and irrigation on soil physical properties, root distribution and water uptake of potatoes (*Solanum tuberosum*). *Soil and Tillage Research* 13, 267–285

Paula, F. L. M., Streck, N. A., Heldwein, A. B., Bisognin, D. A., Paula, A. L., and Dellai, J. (2005). Thermal time of some developmental phases in potato (*Solanum tuberosum* L.). *Ciência Rural* 35, 1034–1042

Pilbeam, C., Simmonds, L., and Kavilu, A. (1995). Transpiration efficiencies of maize and beans in semi-arid Kenya. *Field Crops Research* 41, 179–188

Portmann, F., Siebert, S., and Döll, P. (2010). MIRCA2000 - Global monthly irrigated and rainfed crop areas around the year 2000: A new high-resolution data set for agricultural and hydrological modeling. *Global Biogeochemical Cycles* 24

Porwollik, V., Müller, C., Elliott, J., Chryssanthacopoulos, J., Iizumi, T., Ray, D. K., et al. (2017). Spatial and temporal uncertainty of crop yield aggregations. *European Journal of Agronomy* 88, 10–21

Ramirez-Villegas, J., Koehler, A.-K., and Challinor, A. J. (2017). Assessing uncertainty and complexity in regional-scale crop model simulations. *European Journal of Agronomy* 88, 84–95

Raymundo, R., Asseng, S., Prassad, R., Kleinwechter, U., Concha, J., Condori, B., et al. (2017). Performance of the SUBSTOR-potato model across contrasting growing conditions. *Field Crops Research* 202

Richner, W., Soldati, A., and Stamp, P. (1996). Shoot-to-root relations in field-grown maize seedlings. *Agronomy Journal* 88, 56–61

Robertson, M. and Fukai, S. (1994). Comparison of water extraction models for grain sorghum under continuous soil drying. *Field Crops Research* 36, 145–160

Ruane, A. C. and McDermid, S. P. (2017). Selection of a representative subset of global climate models that captures the profile of regional changes for integrated climate impacts assessment. *Earth Perspectives* 4, 1–20

Sanchez, B., Rasmussen, A., and Porter, J. R. (2014). Temperatures and the growth and development of maize and rice: a review. *Global Change Biology* 20, 408–417. doi:10.1111/gcb.12389. Times Cited: 3 3

Sands, P., Hackett, C., and Nix, H. (1979). A model of the development and bulking of potatoes (*Solanum tuberosum* L.) I. Derivation from well-managed field crops. *Field Crops Research* 2, 309–331

Setiyono, T., Weiss, A., Specht, J., Bastidas, A., Cassman, K. G., and Dobermann, A. (2007). Understanding and modeling the effect of temperature and daylength on soybean phenology under high-yield conditions. *Field Crops Research* 100, 257–271

Smit, A. L. and Groenwold, J. (2005). Root characteristics of selected field crops: Data from the Wageningen Rhizolab (1990-2002). *Plant and Soil* 272, 365–384. doi:10.1007/s11104-004-5979-1

Spaeth, S. and Sinclair, T. (1985). Linear increase in soybean harvest index during seed-filling. *Agronomy Journal* 77, 207–211

Stackhouse, P. W. (2011). Surface meteorology and solar energy

Stalham, M. and Allen, E. (2001). Effect of variety, irrigation regime and planting date on depth, rate, duration and density of root growth in the potato (*Solanum tuberosum*) crop. *The Journal of Agricultural Science* 137, 251–270

Steiner, J. L., Howell, T. A., and Schneider, A. D. (1991). Lysimetric evaluation of daily potential evapotranspiration models for grain sorghum. *Agronomy Journal* 83, 240–247

Streck, N. A., de Paula, F. L. M., Bisognin, D. A., Heldwein, A. B., and Dellai, J. (2007). Simulating the development of field grown potato (*Solanum tuberosum* L.). *Agricultural and Forest Meteorology* 142, 1–11. doi:10.1016/j.agrformet.2006.09.012

Suleiman, A. and Ritchie, J. (2001). Estimating saturated hydraulic conductivity from soil porosity. *Transactions of the ASAE* 44, 235

Tanner, C. (1981). Transpiration efficiency of potato. *Agronomy Journal* 73, 59–64

Tanner, C. and Jury, W. (1976). Estimating evaporation and transpiration from a row crop during incomplete cover 1. *Agronomy Journal* 68, 239–243

Tanner, C. and Sinclair, T. (1983). Efficient water use in crop production: research or re-search? *Limitations to efficient water use in crop production* , 1–27

Timlin, D., Rahman, S. M. L., Baker, J., Reddy, V. R., Fleisher, D., and Quebedeaux, B. (2006). Whole plant photosynthesis, development, and carbon partitioning in potato as a function of temperature. *Agronomy Journal* 98, 1195–1203. doi:10.2134/agronj2005.0260

van Bussel, L. G., Grassini, P., Van Wart, J., Wolf, J., Claessens, L., Yang, H., et al. (2015). From field to atlas: Upscaling of location-specific yield gap estimates. *Field Crops Research* 177, 98–108

Van Heerden, P. D., Tsimilli-Michael, M., Krüger, G. H., and Strasser, R. J. (2003). Dark chilling effects on soybean genotypes during vegetative development: parallel studies of CO2 assimilation, chlorophyll a fluorescence kinetics O-J-I-P and nitrogen fixation. *Physiologia Plantarum* 117, 476–491

Van Keulen, H. and Stol, W. (1995). Agro-ecological zonation for potato production. In *Potato ecology and modelling of crops under conditions limiting growth* (Springer)

Vos, J. and Biemond, H. (1992). Effects of nitrogen on the development and growth of the potato plant. 1. Leaf appearance, expansion growth, life spans of leaves and stem branching. *Annals of Botany* 70, 27–35

Vos, J. and Groenwold, J. (1989). Genetic differences in water-use efficiency, stomatal conductance and carbon isotope fractionation in potato. *Potato Research* 32, 113–121. doi:10.1007/BF02358219

Walker, G. (1986). Transpiratation efficiency of field-grown maize. *Field Crops Research* 14, 29–38

Watson, J., Challinor, A. J., Fricker, T. E., and Ferro, C. A. (2015). Comparing the effects of calibration and climate errors on a statistical crop model and a process-based crop model. *Climatic Change* 132, 93–109

Weedon, G. P., Balsamo, G., Bellouin, N., Gomes, S., Best, M. J., and Viterbo, P. (2014). The WFDEI meteorological forcing data set: WATCH Forcing Data methodology applied to ERA-Interim reanalysis data. *Water Resources Research* 50, 7505–7514

Wolf, S., Marani, A., and Rudich, J. (1990). Effects of Temperature and Photoperiod on Assimilate Partitioning in Potato Plants. *Annals of Botany* 66, 513–520

Yang, H., Dobermann, A., Lindquist, J. L., Walters, D. T., Arkebauer, T. J., and Cassman, K. G. (2004). Hybrid-maize—a maize simulation model that combines two crop modeling approaches. *Field Crops Research* 87, 131–154

Zhou, Z., Andersen, M. N., and Plauborg, F. (2016). Radiation interception and radiation use efficiency of potato affected by different N fertigation and irrigation regimes. *European Journal of Agronomy* 81, 129–137